International Journal of Pharmaceutics: X 5 (2023) 100159

Contents lists available at ScienceDirect

International Journal of Pharmaceutics: X

journal homepage: www.sciencedirect.com/journal/international-journal-of-pharmaceutics-x

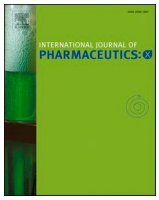

Additive manufacturing technologies with emphasis on stereolithography 3D printing in pharmaceutical and medical applications: A review

Preethi Lakkala [a,1], Siva Ram Munnangi [a,b,1], Suresh Bandari [a], Michael Repka [a,b,*]

[a] Department of Pharmaceutics and Drug Delivery, School of Pharmacy, The University of Mississippi, University, MS 38677, USA
[b] Pii Center for Pharmaceutical Technology, The University of Mississippi, University, MS 38677, USA

ARTICLE INFO

Keywords:
Additive manufacturing
Stereolithography
Photocurable polymers
Photopolymerization
Personalized medicine

ABSTRACT

Three-dimensional (3D) printing or Additive Manufacturing (AM) technology is an innovative tool with great potential and diverse applications in various fields. As 3D printing has been burgeoning in recent times, a tremendous transformation can be envisaged in medical care, especially the manufacturing procedures leading to personalized medicine. Stereolithography (SLA), a vat-photopolymerization technique, that uses a laser beam, is known for its ability to fabricate complex 3D structures ranging from micron-size needles to life-size organs, because of its high resolution, precision, accuracy, and speed. This review presents a glimpse of varied 3D printing techniques, mainly expounding SLA in terms of the materials used, the orientation of printing, and the working mechanisms. The previous works that focused on developing pharmaceutical dosage forms, drug-eluting devices, and tissue scaffolds are presented in this paper, followed by the challenges associated with SLA from an industrial and regulatory perspective. Due to its excellent advantages, this technology could transform the conventional "one dose fits all" concept to bring digitalized patient-centric medication into reality.

1. Introduction

The advancements in the pharmaceutical field have accelerated the development of novel active pharmaceutical ingredients (API), most of which are hydrophobic with low bioavailability and a narrow therapeutic window (Wang et al., 2021). The conventional dosage forms that follow the "one-size fits all" rule pose challenges in delivering API's with a narrow therapeutic window (Durga Prasad Reddy and Sharma, 2020; Wen et al., 2015). These dosage forms do not consider the pharmacokinetic variability, especially in pediatric and geriatric patients, often leading to either subtherapeutic action or adverse effects caused by underdose and overdose, respectively (Menditto et al., 2020). As a result, there is a growing demand for the development of pharmaceutical formulations intended to deliver API within the therapeutic range. The use of 3D printing helps in formulating the API with a narrow therapeutic index, leading to precise doses (Seoane-Viaño et al., 2021). Furthermore, conventional dosage forms' limited drug loading capacity restricts its scope in long-acting formulations. However, the 3D-printed drug-eluting systems can incorporate large quantities of the drug and control the drug release over a period, which has gained attention over the decades (Wang et al., 2021).

3D printing, also known as additive manufacturing (AM), is a printing technology that builds objects layer by layer, replicating the computer-aided design (CAD) model. Under supremacy in precision, high drug-loading, and producing complex structures, this technology is highly capable of addressing the limitations associated with conventional dosage forms and producing effective personalized medicines and medical devices (Xu et al., 2021a). It is often observed that the marketed formulation is crushed or broken manually to adjust the dose for pediatric and geriatric use. This may result in inappropriate dosing and reduces patient compliance, which can be combated using 3D printing technology to tailor patient-specific dose (Chen et al., 2020). In addition to the several advantages mentioned, AM technology is used to develop micro-scale drug delivery systems like microneedles. It is also capable of producing dosage forms with high drug loading, which cannot be achieved through conventional techniques due to the bulkiness and tableting constraints. Despite possessing various advantages that benefit humankind, the AM technique is constrained industrially due to its low

Abbreviations: SLA, Stereolithography; AM, Additive manufacturing; API, Active Pharmaceutical Ingredient; JT Printing, Jet printing; FDM, fused deposition modeling; SLS, Selective laser sintering.

* Corresponding author at: Pii Center for Pharmaceutical Technology, Pharmaceutics and Drug Delivery, University of Mississippi, MS 38677, USA.
E-mail address: marepka@olemiss.edu (M. Repka).

[1] Authors contributed equally.

https://doi.org/10.1016/j.ijpx.2023.100159
Received 19 December 2022; Received in revised form 31 December 2022; Accepted 2 January 2023
Available online 3 January 2023

manufacturing speed compared to conventional manufacturing processes, a limited number of pharmaceutically accepted printing materials, and inefficiency in producing large batches (Zhang et al., 2018). However, the recent advancements in this field enable this technique to overcome these problems. For instance, in 2015, Spritam® (levetiracetam), the first FDA-approved 3D printed tablet was produced using "ZipDose®" technology that works by exuding binder solution onto API-excipient powder (Hsiao et al., 2017).

3D printing or AM technology is an extensive field that classifies into Material extrusion, Vat Photopolymerization, Powder Bed Fusion, Material Jetting, Binder Jetting, Direct Energy Deposition, and Sheet lamination as per the ISO (International Organization for Standardization)/ASTM (American Society for Testing and Materials) (Alexander et al., 2021). Vat photopolymerization is superior to other 3D printing technologies when it comes to creating complex structures with high speed, resolution, and precision. SLA falls under vat photopolymerization technology that uses light irradiation in the form of a laser to initiate photopolymerization in a vat of liquid resin to form solid objects, which gives it a high spatial resolution, with a layer thickness as low as 1 μm. Since its inception, SLA has been well established in several industries, including but not limited to, aerospace, automotive, fashion, jewelry making, and water filtration. It has great potential to establish itself in the medical and pharmaceutical fields to develop personalized medicines, drug-eluting devices, and surgical tools. (Deshmane et al., 2021).

This paper presents an overview of the various 3D printing technologies, mainly delineating SLA and its apparatus, orientation of printing, polymers used for printing, applications in the pharmaceutical industry, and the challenges related to printing and regulatory bodies.

2. A glimpse of various 3D printing technologies

2.1. Jet printing (JT printing)

A typical jet printer is comprised of a print head with thousands of minute pores that fabricate the desired 2D or 3D structure by depositing the ink droplets onto the substrate (base platform) in a layer-by-layer fashion. In pharmaceutical applications, "ink" is defined as the drug dissolved/dispersed in a polymer/resin/solvent or binder solution. The surface tension, viscosity, and volatility of the ink play a vital role in the ideal functioning of JT printing (Chou et al., 2021). As per ISO/ASTM, Binder Jetting and Material Jetting AM technologies use the jet printing mechanism to print the 3D object. In Binder Jetting printers, the print head sprays the liquid agents (usually binding agent solution) selectively as per the CAD design onto powder particles followed by the evaporation of solvent or chemical reactive curing according to the requirement, finally leading to the joining of powder particles. In contrast, with Material Jetting printers, the print head deposits droplets of melted material or photocurable material containing media onto a build platform, where each layer is solidified or cured (Alexander et al., 2021).

Based on the type of technology used to control ink flow during the printing process, this system is categorized into continuous JT (C-JT) and drop-on-demand JT (DOD-JT) printing. C-JT uses high-pressure pumps to ensure the continuous propelling of the ink through the nozzle (Prasad and Smyth, 2015). Wherein a stream of droplets passes through an electrostatic field, which induces an electric charge onto the droplets. Subsequently, the charged droplets are deflected from the mainstream at a specific angle to land on the printing surface, forming the desired pattern (Chou et al., 2021). Volatile solvents are usually preferred in the preparation of ink, which aids in the rapid solidification of a printed structure due to the quick evaporation of the solvent. However, restricted use of solvents and a lower printing resolution limit the use of C-JT printing in pharmaceutical applications (Scoutaris et al., 2016).

On the other hand, DOD-JT printing uses pressure pulses to create smaller droplets than those formed in C-JT, giving rise to high accuracy, precision, and greater resolution (Jacob et al., 2020). There are mainly two types of DOD-JT technologies based on the process involved in generating a pressure pulse, namely thermal and piezoelectric (Park et al., 2019). Thermal DOD-JT has a resistor in the ink chamber that heats up (350–400 °C) rapidly upon receiving the electric signals, creating a vapor bubble that forces the ink down the nozzle and then collapses, creating negative pressure in the reservoir, which aids in drawing the ink from the ink chamber. Due to the resistor's ability to attain high temperatures swiftly, the risk of thermal degradation is lowered. Instead, this technology requires the use of highly volatile solvents because of their rapid vaporability, thus aiding in the formation of vapor bubble (Smith and Morrin, 2017). At the same time, piezoelectric DOD-JT employs a ceramic piezoelectric element to create mechanical movement upon the application of an electric signal. The mechanical movement, in turn, leads to a pressure wave pushing the ink out of the nozzle (Daly et al., 2015). This system allows more control over the droplet formation and doesn't require higher temperatures and a highly volatile solvent to create bubbles. These advantages make this system more feasible and ideal in pharmaceutical applications (Sumerel et al., 2006).

Based on the mode of deposition of the ink, DOD-JT is further divided into drop-on-drop deposition and drop-on-solid deposition. In the drop-on-drop deposition, droplets of ink ejected from the printing nozzle deposit one on the other, forming a solid layer upon evaporation of the solvent. In drop-on-solid deposition, the powder is spread uniformly on the platform, and the binder solution (ink) is sprayed on the powder layer. This process is repeated by lowering the platform until desired mass of the 3D structure is obtained (Goole and Amighi, 2016). These systems are advantageous in developing highly porous materials like oral-dispersible tablets.

2.2. Material extrusion systems

Material extrusion systems are the ones in which a 3D object is fabricated by selectively dispensing the printing material (Ink), which is usually a fusion of drug, excipients, and binder through a nozzle or orifice. These systems uses computer-spatially-controlled methods to disperse the ink through the nozzle and deposit it in a layer-by-layer fashion to obtain the desired 3D structure (Lewis and Gratson, 2004). There are two types of extrusion-based systems, namely pressure-assisted micro-syringes (PAMS) and fused deposition modeling (FDM), classified based on the type of printing material (Ink) used and the method involved in its preparation.

PAMS is incorporated with a viscous semi-liquid printing material (ink), that extrudes through a syringe to generate a predefined 3D structure (El Aita et al., 2020). This system uses compressed air as a driving force to expel the material through the syringe. The additives and solid loading affect the rheological properties of the ink, which is a critical attribute for obtaining reproducibility. The major drawback of this system is the use of solvents, like the ones encountered in IKJT systems (Goole and Amighi, 2016).

Discussing the FDM technology, the drug-incorporated thermoplastic polymer filament is passed through a 3D printing nozzle, where the filament melts and is deposited layer-by-layer to form the desired 3D structure (Chia and Wu, 2015). As the drug-loaded filament undergoes melting both during filament formation and in the print head, the polymer's melting point should preferably be low to avoid drug degradation. In addition to the low melting point, the polymer melt viscosity should be optimum for its extrusion and for building a 3D structure. Generally, these drug-loaded filaments are prepared by a solvent-free process using hot-melt extrusion (HME), a green technology. In the preparation of a filament, the drug along with polymer, and other additives are melted together in an extruder, homogenized, and extruded through a nozzle to form a filament (Bandari et al., 2021). Typical factors that need to be monitored during the FDM process are the temperature of the print head, in-fill density, extrusion speed, and layer

thickness. This system is economically friendly, easily reproducible, and provides accurate dosing by modifying the print volume of the drug delivery substrate. The release profile of the formulation can easily be modified just by adjusting the in-fill density and geometry of the drug delivery system. During the filament formation in the HME, the polymer matrix allows the conversion of the crystalline drug into an amorphous form, eventually leading to enhanced solubility of poorly soluble drugs (Chai et al., 2017). However, the limited availability of biodegradable thermoplastic polymers, low printing resolution, and the inability to use thermolabile drugs hinders the applications of this technology.

However, an innovative extrusion-based technology, Melt Extrusion Deposition (MED™) 3D printing, has been introduced recently. In this new technology, the powder feedstocks can directly be incorporated, which then converts into softened/molten substances and then deposits layer-by-layer to form an object with desired internal geometries. This overcomes the disadvantages owing to filament production, wherein the drug is exposed twice to heat and thus increasing the chances of drug-degradation (Zheng et al., 2021).

2.3. Powder bed fusion (PBF)

PBF is a process of selectively fusing the powder particles into a 3D object using thermal energy (*e.g.*, a laser). Selective Laser Sintering (SLS) is categorized under the PBF type of printing technology and is being used extensively in pharmaceuticals. SLS works by sintering finely powdered particles to form a 3D structure by selective exposure to a high-energy laser. This system comprises a spreading roller (re-coater), powder feed chamber, powder build chamber, build platform, and a laser source with high power and scanning mechanism (Charoo et al., 2020). A 3D object is formed by mimicking the CAD model that is imported to the SLS printer through software. The printing process begins immediately after the information is communicated to the printer. The process begins by feeding the powder into the powder feed chamber, where the spreading roller spreads the powder onto the build platform. Subsequently, a high-power laser beam focuses on the uniformly spread layer in accordance with the CAD design, sintering the particles and solidifying them to create a two-dimensional layer. The build platform then descends to a height equal to layer thickness, thenceforth a second layer is spread on the first layer and is sintered to it using the laser. This process is repeated until the desired 3D structure is formed (Charoo et al., 2020). After the printing process is finished, the printer cools down to bring the 3D object to room temperature. Finally, the 3D object is taken out and dusted off to remove powder retention.

The critical process parameters include the bed thickness, temperature, and powder properties like particle density, shape, size, and size distribution. The more considerable difference in particle size distribution can cause significant segregation affecting the sintering process. Also, the powder needs to possess good flowability and a particle size range of 58–180 μm to achieve uniform spreading and compelling sintering of particles (Awad et al., 2020). Despite its advantages, SLS possesses various challenges like limiting its use for heat-sensitive drugs and being unable to reuse the powder that underwent processing conditions that significantly affect the mechanical properties of the outcome. (Gueche et al., 2021).

2.4. Vat-photopolymerization

Vat photopolymerization 3D printing technology can be defined as the process of fabricating a 3D object by selectively solidifying the liquid photopolymerizable material upon exposure to light. This technology is further categorized into four types based on the light source and its projection onto the photopolymerizable material. These entail 1. stereolithography (SLA), 2. digital light processing (DLP), 3. continuous light interface production (CLIP), and 4. two-photon polymerization (TPP) (Wang et al., 2021).

SLA uses a computer-controlled UV-laser beam for photopolymerization. A single laser beam focuses on the vat of liquid resin to selectively cure layer-by-layer to produce a 3D object. The use of a laser beam enables the fabrication of objects with high precision and a smooth surface finish. The pharmaceutical and medical applications of this technology are mentioned in detail in the further sections.

The DLP system uses a digital projector screen to project the light comprising small pixels (rectangular cubes) of a whole cross-sectional layer of objects onto the photopolymerizable material. The entire cross-sectional area solidifies upon the projection of light. The resulting 3D object is composed of small rectangular cubes called voxels giving it a rough surface finish. Due to the polymerization of the whole cross-section at once, these systems print the objects at a faster rate compared to SLA. However, in both SLA and DLP systems, the solidified layer peels off from the base of the vat, resulting in increased fabrication time (Zhao et al., 2020). Some examples of the dosage forms and drug-eluting devices fabricated using this technology include, fluticasone eluting esophageal-targeted 3D rings (pre-loaded and post-loaded) fabricated by Prasher et al. (2021), by employing a top-down DLP printer (Gizmo® 3D printer). The dimensions of fabricated ring were 24 mm outer diameter (OD), 20 mm height (H), and 2.5 mm cross section (CS). The *in vitro* dissolution studies demonstrated that altering the crosslink density of resin formulations varies the drug release kinetics. Fluticasone *in vitro* drug release was optimized to a target release of 1 mg/day. *In vivo* pharmacokinetic studies in a porcine model revealed a high local level of fluticasone in esophageal tissue that lasted between 1 and 3 days, with little systemic absorption in plasma. This approach demonstrates the potential pathways to treat several esophageal conditions (Prasher et al., 2021). Xu et al. (2021a), fabricated two drug loadings of dexamethasone (10% *w*/w and 20% *w*/w) punctual plugs using a DLP 3D printer (Titan2 HR, Kudo3D Inc.), for controlled drug delivery to the eye. Different ratios of PEGDA and PEG 400 were used as printing material. These punctual plugs (length ranging from 1.0 to 2.0 mm, diameter ranging from 0.2 to 1.0 mm, and core diameter of 0.5 mm) were evaluated for *in vitro* drug release kinetics using an in-house method that mimics the subconjunctival space, called the flow rig model. The results revealed that the drug was released for up to 7 days from the punctual plug developed with 20% w/w PEG 400 and 80% w/w PEGDA, whereas the drug was released over 21 days from the punctual plug comprising 100% PEGDA. This research demonstrates the efficiency of DLP in developing various extended release personalized ocular devices (Xu et al., 2021b). Further, Rodríguez-Pombo et al. (2022), introduced a novel volumetric 3D printing technology, which is an advancement and is superior to DLP, intended to rapidly fabricate medicines. They fabricated torus-shaped (11 mm diameter x 4 mm height, and a central hole with a 3 mm diameter) paracetamol-loaded 3D tablets (Printlets™) within 7–17 s, using a volumetric printer (FabRx Ltd., UK) that utilized a DLP projector. Seven mirrors were positioned at different angles in front of the projector to focus UV light onto the resin from 3 different directions (left side projection, right side projection, and bottom projection). The printing material was composed of a crosslinking monomer (PEGDA), photoinitiator (lithium phenyl-2,4,6-trimethylbenzoylphosphinate (LAP)), and diluents (water or PEG300), and six different resin formulations were prepared using different ratios of these components. This new technology is a promising tool for the rapid production of personalized medicines and medical devices (Rodríguez-Pombo et al., 2022).

Like DLP systems, the CLIP system also projects light comprising small pixels of whole cross-sectional layers of objects onto the photopolymerizable material. However, unlike the digital projector screen in DLP systems, CLIP utilizes more advanced digital projectors based on light-emitting diode (LED) or laser. CLIP printers possess an oxygen-permeable layer creating a dead zone above the base of the vat, allowing continuous printing of the object instead of layer-by-layer fabrication as observed in SLA and DLP printers (Quan et al., 2020). The oxygen-permeable layer consists of oxygen, which reacts with monomers (monomers that undergo free radical photopolymerization) to

form peroxy radicals, thus inhibiting photopolymerization. The peroxy radicals are more stable and do not easily restart the polymerization (O'Brien and Bowman, 2006). Therefore, the resin continuously flows between the polymerized material and base of the vat, thus readily available for polymerization. This continuous polymerization increases the printing speed by 25–100 times as compared to SLA and DLP systems (Hahn et al., 2020). However, CLIP requires low-viscosity resins. Also, the oxygen permeable layer is highly expensive (Quan et al., 2020). Here are a few examples of the systems fabricated using CLIP. Hagan et al. (2022) created a 3D printed implantable device containing cisplatin and/or paclitaxel, using a Carbon3D S1 prototype CLIP printer. The implant was made up of two layers: an inert base layer with a thickness of 300 μm and a drug-infused layer with a thickness of 400 μm and 1.5 mm arrowheads on the top. *In vivo* efficacy studies on mice, successfully reduced the local recurrence of tumor post-surgery (Hagan et al., 2022). Similarly, the microneedles for transdermal vaccine delivery were fabricated by Caudill et al. (2021). The group used a Carbon3D S1 prototype CLIP printer to create microneedle patches, which were then coated with vaccine antigens and adjuvants. The patch has 700 μm long microneedles in a 10*10 array on a 10*10 mm patch. The developed microneedles successfully induced a potent immune response in a non-invasive manner comparable to a subcutaneous bolus injection (Caudill et al., 2021).

TPP uses a near-infrared femtosecond laser beam for photopolymerization. In this technique, two laser (photon) beams are projected simultaneously to solidify the resin and create a predefined 3D structure. It has a very high resolution capable of reaching 100 nm. Recently, TPP achieved sub-100 nm spatial resolution by employing a radical quenching mechanism (Lee et al., 2008). This technique is highly useful in printing microstructures with utmost precision (Wang et al., 2021). For instance, Plamadeala et al. (2019) developed microneedles for transdermal drug/vaccine administration. The Workshop of Photonics® provided the group with a TPP printer. The MNs were designed as 210 mm tall pyramids with square bases, 160 mm long sides, and 10 mm thick walls. The sides of the microneedles were embellished with microstructures with a base width of 10 mm, tip height of 5 mm, and a distance of 30 mm was maintained between two consecutive rows. *Ex vivo* tests on human skin demonstrated their ability to deliver the drug/vaccine coated on the surface without microneedle breakage (Plamadeala et al., 2019).

Lastly, in an innovative and intriguing work by Xu et al. (2021b), a smartphone was used in fabricating personalized 3D printed tablets (warfarin sodium printlets). In this technology, the light emitted from the smartphone's screen was used to photopolymerize the liquid resin to obtain a solid structure. Various personalized geometries of warfarin-loaded printlets were successfully fabricated (caplet, triangle, diamond, square, pentagon, torus, and gyroid lattices) and these showed sustained drug release. This system allows fabricating one's own medicines at home and during emergencies, in an economical way (Xu et al., 2021d).

3. Stereolithography (SLA)

Among various potential technologies for 3D printing, SLA is the first and oldest, yet it delivers complex geometries and smooth-surfaced objects owing to its high printing resolution and is widely used. In 1984, Charles Hull invented and patented the first 3D printing technology using SLA, which belongs to vat photopolymerization. The term SLA is derived from two words, stereo(solid) and (photo)lithography, which implies, the form of 'writing with light'. The materials used in SLA are photopolymerizable, implying that these materials solidify upon exposure to light, specifically UV light. The shape and size of the object are controlled by selectively exposing the light using a spatially controlled laser (Hull and Arcadia, 1984). The UV irradiation used for photopolymerization is low-powered and usually generated from He-Cd/Nd: YVO4 laser (Bikas et al., 2016).

3.1. Mode of UV light exposure in SLA apparatus

SLA accommodates a laser projector, which focuses the laser beam on a liquid resin to photopolymerize layer by layer to form a 3D object. The resolution with which an object is printed is based on the diameter of the laser beam. A laser directs the light to two mirror galvanometers, which move in X and Y planes. These mirrors direct the light to the correct coordinates focusing the light upward through the base platform onto the resin/photopolymerizable material, curing a layer of resin/photopolymerizable material. The fabrication time is more because of the limited surface area of resin that is exposed to the laser beam and due to the layer-by-layer fabrication (Manapat et al., 2017; Mitteramskogler et al., 2014).

3.2. Components of SLA apparatus

A typical SLA apparatus comprises five key elements: build platform, optics, vat, recoater, and a control system as depicted in Fig. 1A (Zakeri et al., 2020). The vat (tank) accommodates the liquid resin used for printing and is integrated with the refill system connected to the resin tank (source of liquid resin) situated outside the apparatus. The liquid resin used is relatively viscous, making its surface in the vat bumpy, for which a recoater (mixer) is used for uniformly distributing the resin to obtain a flat and even surface. The build platform is the one on which a 3D object is fabricated, and it is accompanied by an elevator to facilitate vertical movement during the printing process (Gibson et al., 2015; Zakeri et al., 2020). Further, optics consists of the light source, an acoustic, optical modulator for swiftly switching on and off the light source, a *Z*-focus lens used for focusing the laser beam over the resin surface, and two inertia galvanometers for scanning the projection of the laser beam. Lastly, the control system comprises a process controller, beam controller, and environment controller, which respectively control the sequence of machine operations, scanning speed along with the focal depth of the laser beam, and temperature and humidity of the vat chamber (Gibson et al., 2015; Zakeri et al., 2020).

3.3. Orientation of printing in SLA apparatus

The SLA 3D printing apparatus is categorized into two types based on the orientation of printing and the location of the light source, and its direction of projection. They are known as "Top-Down" and "Bottom-Up" 3D printers (Zakeri et al., 2020).

In the top-down SLA apparatus Fig. 1A, the light source used for curing the photopolymerizable material is situated above the vat. During the process of printing, the build platform is immersed into the vat of liquid resin to a depth of one layer thickness, which gets cured/solidified by UV irradiation from the light source positioned above (Huang et al., 2020a; Taormina et al., 2018). Each time, the build platform moves downward on Z-axis to a depth of one layer thickness, creating space for the resin to spread evenly and cure over the previous layers. This process is repeated until all the layers are built to form a 3D object. This type of setup suffers from several limitations. Firstly, the downward movement and immersion of the build platform into the resin create a disturbance on the surface of the resin, which consumes time for attaining equilibrium of the surface. Secondly, though equilibrium is attained over the resin, the flat surface cannot be achieved, which is restored with the help of a recoater (mixer) which again is a time-consuming process. The entire process reduces the overall production efficiency of the apparatus (Kozhevnikov et al., 2020). Therefore, low viscosity resins are recommended as they consume less time to restore their equilibrium. Lastly, the uppermost uncured layer is always in contact with oxygen, which inhibits the photopolymerization of certain resins, resulting in an improper curing (Ligon et al., 2017). Moreover, this setup requires large quantities of resin.

In the bottom-up SLA apparatus, the light source is situated at the bottom of the resin tank, from which the light is projected upwards,

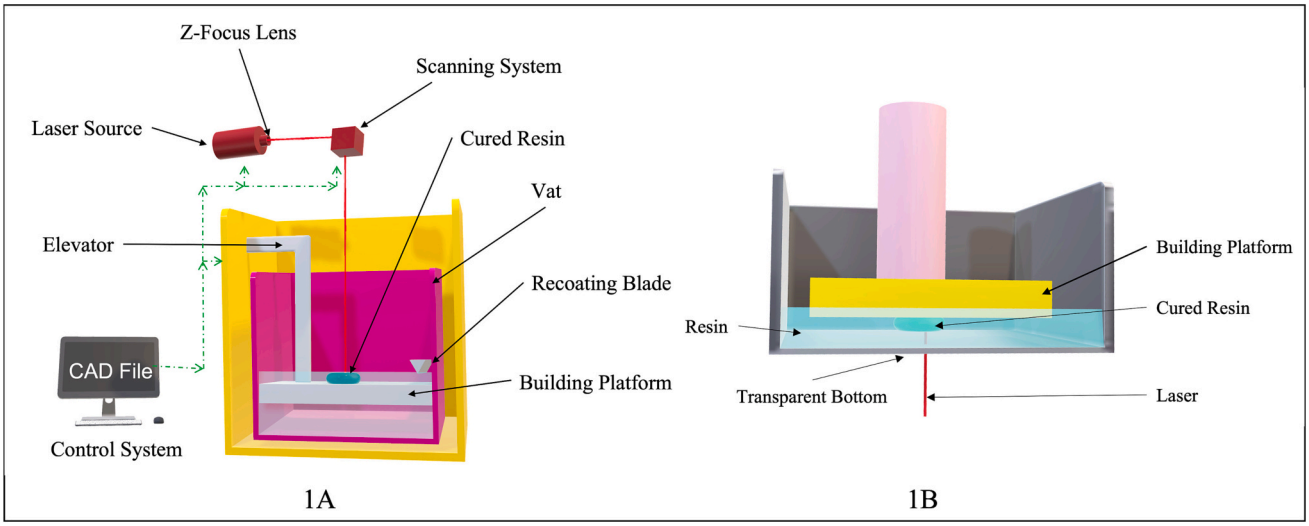

Fig. 1. 1A - Schematic representation of SLA (Top-Down Approach); 1B - Schematic representation of SLA (Bottom-Up Approach).

initiating the photopolymerization of resin, as shown in the Fig. 1B (Taormina et al., 2018). This setup requires a vat with non-sticky and transparent film at the bottom for easy detachment of the cured layer (Pan et al., 2017). This system uses a shallow vat and requires less quantity of resin for printing. The build platform immerses into resin, maintaining a gap of one layer thickness above the transparent film, (vat bottom) which eventually solidifies on exposure to UV light. Once the resin layer is cured, the build platform raises vertically upward again to a height of one layer thickness between the previously cured layer and the transparent film at the bottom, creating a space for the new layer to be formed (Yogesh et al., 2020). The newly formed layer detaches from the vat bottom as the build platform move upwards, which can lead to sticking of the layer to transparent film resulting in improper surface finish. This limitation can be addressed by coating the vat bottom with either teflon or silicon films to easily remove the solidified resin layer (Ligon et al., 2017; Tumbleston et al., 2015). Unlike in the top-down process, the bottom-up process has no contact of the newly forming layer with oxygen, which improves the photopolymerization and curing rate (Lian et al., 2017). The thickness of each layer is maintained precisely in this approach as it is controlled by the vertical movements of the built platform, not by the fluid motion of the resin. This bottom-up process has limitations owing to its low volume holding capacity of the vat and laborious removal of the 3D print from the built platform. Therefore, this system allows the printing of only the smaller 3D structures. Also, as the 3D structure builds upside down, hanging from the base of the built platform, it must overcome the gravitational pull (He and Song, 2018). So, to ensure the 3D structure is properly intact to the base and to prevent it from falling off due to the gravitational pull, it must be accompanied by the "supports". However, these "supports" has to be removed from the structure once the printing process is finished, which is a tedious and painstaking process, and it might leave marks on the surface of the object (He et al., 2019).

4. Materials used in SLA

Polymerization is the process in which the short-chain monomers/oligomers cross-link to give long-chain macromolecules. Various stimulation methods like physical, chemical, and irradiation, can be used to induce cross-linking of monomers. The SLA 3D printing technology uses light irradiation as a source of stimuli to induce photopolymerization of the monomers/oligomers present in the liquid resin to obtain solid macromolecules. The photopolymerization of resin mainly depends on the "quantity" and "quality" of the light used. The quantity of light is defined by the exposure time required to complete the photopolymerization of the resin. In contrast, the quality of light is defined by the wavelength being used to achieve photopolymerization. In general, wavelengths in the range of the UV (200–500 nm) and visible (400–700 nm) spectra are used. However, the monomers are incapable of generating reactive species to undergo photopolymerization upon light irradiation. Therefore, an additional component called "photo-initiator" is used for generating reactive species. These reactive species attack and modify the monomers' functional groups, leading to polymer formation. In addition to these components, several other substances like dispersion agents, drugs, and plasticizers may be added to the printing material (ink) depending on the intended properties of the final 3D object (Zakeri et al., 2020).

4.1. Polymers

A polymer is a macromolecule composed of smaller repeating subunits called monomers/oligomers. In the SLA 3D printing process, the resin (ink) is composed of photosensitive monomers/oligomers capable of undergoing photopolymerization on exposure to light to form polymers. Therefore, the photopolymers are of utmost importance and are vital components in the SLA. Nevertheless, the lack of FDA-approved biocompatible and biodegradable photosensitive polymers limits the broad applications of SLA. However, recent times have witnessed many advancements that lead to the development of various biocompatible photopolymers that are suitable to be used in SLA technology. Some of the examples are polyethylene glycol diacrylate (PEGDA) (Seo et al., 2017), polyethylene glycol dimethacrylate (PEGDMA) (Burke et al., 2020), poly (2-hydroxyethyl methacrylate) (pHEMA) (Steinbach et al., 2020) and polypropylene fumarate (PPF) as shown in Fig. 2 (Lee et al., 2007). Though there are various commercially available resins for use in SLA, their compositions are not disclosed. The photopolymers undergo photopolymerization through two mechanisms, namely the free radical and the cationic systems. The acrylates and thiol-based resins undergo free radical photopolymerization, while epoxy resins undergo cationic photopolymerization (Bagheri and Jin, 2019).

The monomers of methacrylates and acrylates are widely employed in pharmaceutical applications because of their fast reaction rates, flexible mechanical properties, and stability. However, these monomers pose a limitation by experiencing volume shrinkage during the photopolymerization, which results in highly brittle 3D objects (Wang et al., 2019). This issue can be mitigated by the introduction of flexible oligomers. For instance, an amalgamation formed by the addition of (methacryloxypropyl)methylsiloxane (MAOMS) to the commercial resin gives rise to siloxane-methacrylate exhibiting enhanced tensile

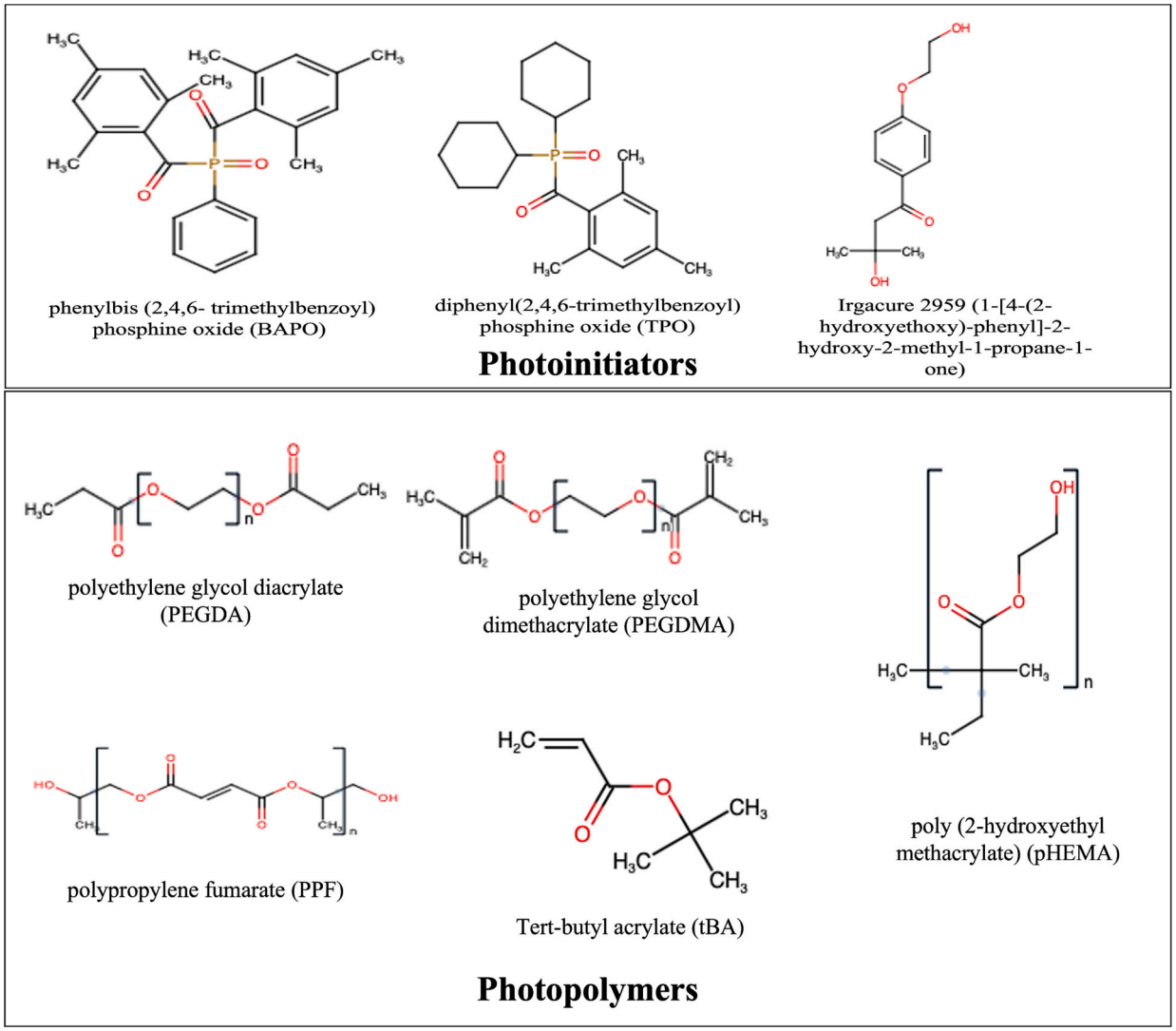

Fig. 2. Structures of some Photoinitiators and Photopolymers used in SLA 3D printing.

toughness, decreased glass transition temperature, tensile strength, and surface energy (Palaganas et al., 2017). Similarly, the hybrids comprising epoxy aliphatic acrylate, aliphatic urethane diacrylate, and isobornyl acrylate exhibit high stretchability/elasticity. The 3D prints formed from these systems can be stretched by about 1100%, which is at least five times more than the commercially available elastomers, allowing temporary deformations during the printing process. These elastomers can self-heal after deformation and can regain 100% of their mechanical strength (Patel et al., 2017). In addition, a group of smart materials called "shape memory" polymers can regain their original shape from a deformed or temporary shape on exposure to external stimuli like temperature, pH, light, and hydration. A material formed by the combination of PGEDA and PGEDMA is an example of a hydration-stimulated shape-memory polymer (Zhao et al., 2018). These systems paved the way for the development of 4D printing, where the fourth dimension represents the dynamic shape transformation over time (Weems et al., 2021). The major limitation concerning acrylate-based polymers is that they are prone to oxygen inhibition, which can be mitigated by adding amines or triphenylphosphine (Bagheri and Jin, 2019). However, the addition may sometimes be incompatible with the commercially available resins and can also cause unwanted effects decreasing the efficiency of the 3D printing and the 3D-print. Furthermore, the methacrylate modification of natural polymers like hyaluronic acid and chitosan can be used for bio-fabrication aiding in tissue repair and regeneration (Raman and Bashir, 2015). This polymerization technique permits the production of a wide variety of bio-degradable hydrogels using synthetic and natural polymers. The resulting hydrogel mostly possesses tunable mechanistic properties, which can further be functionalized with various moieties based on the needs like cell adhesiveness and biodegradability (Pereira and Bártolo, 2015).

The thiol-ene system works by the reaction of thiols with the carbon-carbon double bonds (enes) (Kade et al., 2010). They have the edge over acrylate-based systems in terms of low shrinkage, high biocompatibility, and resistance to oxygen inhibition. Therefore, these systems are highly suitable for fabrication into biocompatible, biodegradable 3D-printed structures (Bagheri and Jin, 2019). The most used thiol monomers are trimethylolpropane tris(3-mercaptopropionate) (TMPMP), pentaerythritol tetrakis (3-mercaptopropionate) (PE-1), and pentaerythritol tetra(3-mercaptopropionate) (PETMP) (Li et al., 2019). Also, due to the ability of these systems to form thioether linkages which in turn form homogenous networks, it is used in building soft materials. Despite these advantages, their application is hindered by a few disadvantages like bad odor and poor shelf-life (Bagheri and Jin, 2019).

Epoxy resins use a cationic photopolymerization mechanism. The commercially available epoxy resins are 3,4 (epoxycyclohexane) methyl 3,4 epoxycyclohexylcarboxylate (EPOX), Bis[2-(3,4-epoxycyclohexyl) ethyl] octamethyltetrasiloxane (BEPOXOMTS) and bisphenol A diglycidyl ether (DGEBA) (Balakrishnan et al., 2020; Huang et al., 2020b;

Sangermano et al., 2010). Besides, 1,4-cyclohexane dimethanol divinyl ether, (CDVE) a vinyl ether, uses a cationic photopolymerization mechanism and is commonly used in SLA (Lapin et al., 1994). These monomers offer lower shrinkage rates than those observed in free-radical polymerization. However, they undergo photopolymerization intensively with a high number of cross-linkable points, increasing the bristliness of the final structure. This can be overcome by decreasing the density of cross-linkable points by adding low concentrations (5–20% *w/w*) of chain transfer agents like polyester and polyether diols (Bagheri and Jin, 2019). Despite various advantages, cationic polymerization is not preferred for biomedical applications for various reasons. Firstly, protonic acid species are produced during photopolymerization, which causes negative effects on cells (Tomal and Ortyl, 2020). Secondly, it is susceptible to moisture (Upul Ranaweera et al., 2015). Nevertheless, combining different reactive monomers or a hybrid of acrylate and epoxy monomers can help regulate the photopolymerization and tuning of the properties of 3D-printed objects (Lee et al., 2017).

4.2. Photoinitiators

The reactive species are necessary for the initiation of monomer/oligomer photopolymerization. However, since the monomers/oligomers cannot produce the necessary reactive species, photoinitiators that can do so are needed. The selection of photoinitiators, usually low-molecular-weight organic compounds, is a key requirement for effective photopolymerization. The photoinitiators are categorized based on the type of reactive species produced after the absorption of UV light. The free radical photoinitiators are used for monomers of methacrylate, acrylate, and thiol. These photoinitiators produce free radical reactive species that react with the monomers giving rise to polymerization. The commonly used free-radical photoinitiators are the derivatives of benzoin, acetophenone, hydroxyalkylphenones, and acylphosphine oxide as shown in Fig. 2. Irgacure 2959 (1-[4-(2-hydroxyethoxy)-phenyl]-2-hydroxy-2-methyl-1-propane-1-one) is one of the widely used free-radical photoinitiators due to its low cytotoxicity but has a limitation of low initiation efficiency. Therefore, the free-radical photoinitiators with better initiation efficiency and biocompatibility were developed, named 2,2′-azobis[2-methyl-*N*-(2-hydroxyethyl) propionamide] (VA-086) and lithium phenyl-2,4,6-trimethylbenzoylphosphinate (LAP). Alongside, the research has been carried out using a variety of free-radical photoinitiators (Fig. 2) like riboflavin, Eosin-Y, diphenyl (2,4,6-trimethylbenzoyl) phosphine oxide (TPO) and phenyl-bis (2,4,6-trimethylbenzoyl) phosphine oxide (BAPO), *etc.* (Karakurt et al., 2020; Pereira and Bártolo, 2015; Robles-Martinez et al., 2019). On the other hand, cationic photoinitiators produce acids that react readily with epoxy resins causing photopolymerization. Some examples of cationic photoinitiators are aryl iodonium salts and sulfonium photoinitiators (Bagheri and Jin, 2019). The production of protonic acids by these initiators hinders their biomedical applications (Pereira and Bártolo, 2015). During polymerization, the reactive species decompose the functional groups of monomers producing reactive C═C, which readily react with carbon atoms on other monomers forming a dimer and the chain reaction continues forming a polymer. During this process, the weak van der Waals interactions get replaced by strong covalent bonds causing the liquid resin to transform into a solid structure (Zakeri et al., 2020).

5. Applications of SLA in pharmaceuticals and medical devices

A wide variety of novel and innovative products have been developed using SLA. These products can be developed either by incorporating the drug in the polymer solution or directly into the printed product, as shown in Fig. 3. The release process is by diffusion and erosion, respectively. Some of the applications include the development of tablets, microneedles, bio-medical scaffolds, dental prosthetics, medical devices, etc. Various types of pharmaceutical products developed using SLA are mentioned in Table 1.

5.1. Oral solid dosage forms – tablets

The tablets are one of the most convenient dosage forms due to their patient compliance. In recent times, conventional tablet manufacturing is encountering advancements inclined towards developing patient-centric/personalized medication based on the patient's pharmacological profile, age, and gender. Therefore, there is a rising demand for personalized, immediate, and modified-release tablets. The release profiles of the conventionally produced tablets are usually dependent on the polymer and its concentration. In comparison, the 3D printing technology provides the opportunity to modify the drug release by controlling the geometrics of tablets like in-fill density and surface area to volume ratio (Thakkar et al., 2020; Windolf et al., 2021). There are several immediate and modified release tablets that have been produced using SLA. For example, Karakurt et al. (2020) used SLA 3D printing (Anycubic Photon 3D) to fabricate ascorbic acid-loaded solid dosage

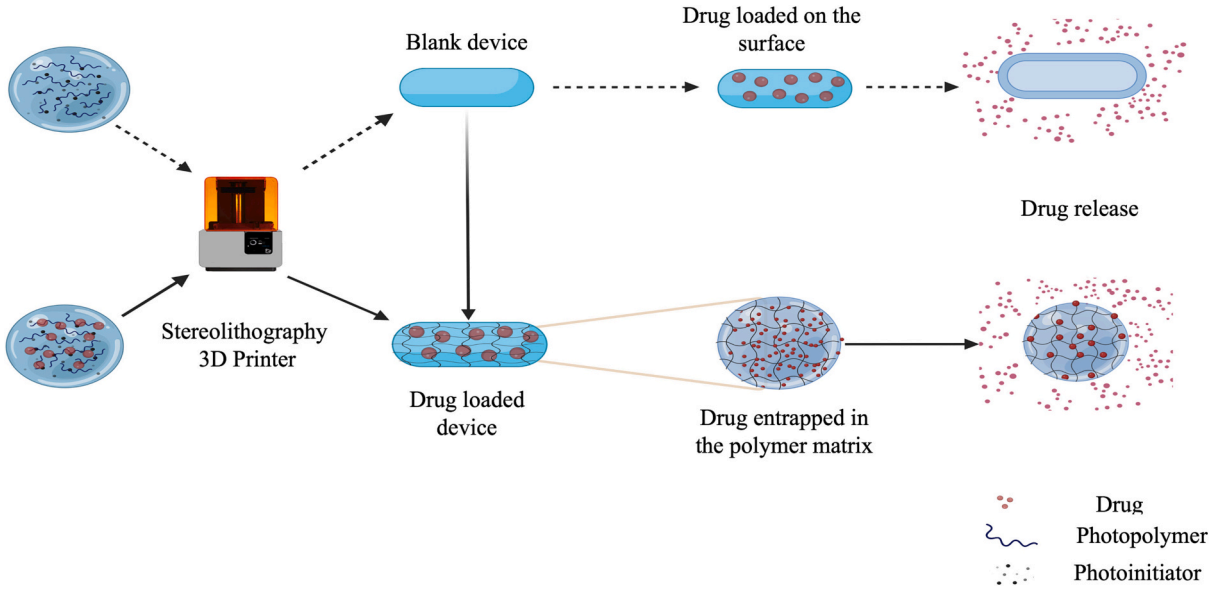

Fig. 3. SLA fabricated 3D-drug delivery systems.

Table 1
Examples of drug delivery systems fabricated using SLA.

Drug	Dosage Form	Excipients		Dimensions	Reference
		Monomer	Photoinitiator		
Paracetamol & 4-aminosalicylic acid	oral modified-release dosage form	polyethylene glycoldiacrylate (PEGDA)	diphenyl(2,4,6-trimethylbenzoyl) phosphine oxide	Torus shape tablets, 11 mm diameter × 4 mm height and The central hole of 3 mm diameter	(Wang et al., 2016)
paracetamol, caffeine, naproxen, chloramphenicol, prednisolone, and aspirin,	polypills	polyethylene glycoldiacrylate (PEGDA)	diphenyl(2,4,6-trimethylbenzoyl) phosphine oxide	cylinder—10 mm diameter and 3 mm height ring—10 mm diameter and 6 mm height	(Robles-Martinez et al., 2019)
Berberine chloride	Nano-composite pills	polyethylene glycoldiacrylate (PEGDA)	diphenyl(2,4,6-trimethylbenzoyl) phosphine oxide	Height- 5 mm Diameter – 7.5 mm	(Choudhury et al., 2021)
Rifampicin	Hollow microneedles (HMNs) array	Dental SG resin		MNs per array- 49 (7*7) Each cubical reservoir with dimensions 13.0 mm × 13.0 mm × 3.5 mm	(Yadav et al., 2021)
Dacarbazine	drug-loaded microneedle arrays	poly(propylene fumarate): diethyl fumarate (50:50)	diphenyl(2,4,6-trimethylbenzoyl) phosphine oxide	The length of microneedle is 700 μm and conical tip of 300 μm. While apex diameter is 20 μm.	(Lu et al., 2015)
Lidocaine hydrochloride monohydrate	Urinary bladder insert	Elastic Resin		Solid Device – 130 mm length and 3 mm diameter Hallow device – 130 mm length, 3 mm outer diameter, 0.5 mm shell thickness	(Xu et al., 2021c)
Implants	Antimicrobial dental implants	Quaternary ammonium methacrylate prepared by incorporating quaternary ammonium groups into diurethanedimethacrylate/glycerol dimethacrylate	Bisacrylphosphine oxide	Different models with various dimentions	(Yue et al., 2015)
	Prosthetic vascular grafts	α,w-polytetrahydrofuranether-diacrylate	Irgacure 184 (1-Hydroxycyclohexyl phenyl ketone)	Inner diameter - 20 μm to 2 mm	(Meyer et al., 2012)
Ciprofloxacin Fluocinolone acetonide	Drug eluting hearing aids	Kudo 3DSR Flexible resin & Kudo 3DSR ENG hard resin		Circular discs – 10 mm diameter * 1 mm height Rectangular slabs – 10 mm*20 mm*1 mm	(Vivero-Lopez et al., 2020)

hydrogels by using a PEGDMA-based polymer system and riboflavin as a photoinitiator. Different geometries [small (15 mm diameter) and large (20 mm diameter) tablet, coaxial annulus tablet (15 mm outer diameter, 10 mm inner diameter), 4-circle pattern (20 mm diameter, 4 holes with 4 mm diameter), and honeycomb pattern(20 mm diameter, hexagonal holes of 4 mm diameter)] with surface area to volume ratios ranging from 0.6 to 1.83 were printed to study the drug release. By conducting drug release studies, they found that the honeycomb and coaxial annulus tablet gels showed higher release rates (Karakurt et al., 2020). In another study by Wang et al. (2016), a 3D-printed tablet of paracetamol (5.69%) and 4-aminosalicylic acid (4-ASA) (5.40%) was developed using SLA (Form 1+ SLA 3D printer). Photopolymer (printing) solution was prepared using polyethylene glycol diacrylate (monomer) and diphenyl (2,4,6-trimethylbenzoyl), while phosphine oxide was the photoinitiator. They fabricated tablets (Shape-torus, 11 mm diameter × 4 mm height, with a central hole of 3 mm diameter) with different properties achieved by adding polyethylene glycol 300 (PEG 300) to the printing solution, and the effect of PEG 300 on drug release kinetics was also evaluated. It was found that the drug dissolution profiles were modified based on the varying concentrations of cross-linkable polymers. In this study, the dissolution rate was decreased with higher ratios of PEGDA, whereas drug release was increased with higher ratios of PEG 300 (Wang et al., 2016).

Similarly, Martinez et al. (2018) printed different geometric shapes (cube, disc, pyramid, sphere, and torus) of tablets containing paracetamol dispersed in PEG using SLA 3D printing (Formlabs 1+ SLA 3D printer). They performed dissolution tests for different geometric shapes by keeping either surface area (SA) constant or surface area/volume ratio (SA/*V*) constant. Test results showed that the tablets with a constant SA/V ratio had the same rate of drug release, whereas constant surface area had different rates of drug release. Tablets with tori shapes showed an increase in dissolution rate with an increase in the SA/V ratio. The results from this work implied that the SA/V ratio has the most significant influence on the drug release kinetics when compared to other geometric parameters. Thus, SLA 3D printing's ability to manufacture personalized dosage forms by controlling geometric parameters was demonstrated (Martinez et al., 2018). Martinez et al. (2018) developed a novel stereolithographic multi-resin 3D printing (Formlabs 1+ SLA 3D printer) method used for fabricating multi-layered constructs (polypills) with different drug concentrations and shapes. They printed a tablet with six active ingredients (paracetamol, caffeine, naproxen, chloramphenicol, prednisolone, and aspirin). Raman microscopy was used to visualize drug distribution from different layers, to confirm if the layers were successfully printed. Dissolution tests showed distinct drug release profiles due to the layer arrangements and drug properties. This work has demonstrated the production of multi-drug therapy (personalized polypills) using SLA 3D printing (Robles-Martinez et al., 2019). Sharma et al. (2022) developed a nanocomposite drug delivery system comprising berberine entrapped nanoparticles immobilized in a 3D printed pill, using SLA (Form 2 SLA printer). The berberine entrapped nanoparticles were incorporated into photopolymerizable biocompatible resin, which is composed of PEGDA as a photocrosslinkable monomer. While TPO was used as a photoinitiator, and PEO as a swelling agent. Electron microscopy revealed successful entrapment of hydrogel nanoparticles within the pills during the SLA process. Sustained release of berberine from 3D printed pill (Diameter – 7.50 mm and Thickness – 5.00 mm) was achieved (Sharma et al., 2022). Thus, these studies demonstrated the potential of SLA 3D printing technology

in developing oral dosage forms (tablets).

5.2. Topical and transdermal dosage forms

Topical and transdermal delivery presents an alternative route for orally degradative drugs and for drugs prone to degrade under the gastric environment and undergo hepatic metabolism. These dosage forms are used for delivering the drugs both locally and systematically. Various types of topical and transdermal delivery systems, like films and microneedles, have been fabricated using this technology. For instance, Choudhury et al. (2021) fabricated polymeric film for berberine (BBR) delivery using SLA 3D printing. The resin solution was prepared using PEGDMA as the photopolymer, PEG 400 for hydrophilicity and penetration enhancement, and TPO as a photoinitiator. BBR was incorporated into the resin solution, and topical films (thickness – 1 mm and sides – 25 mm) were printed using an inverted SLA 3D printer (Form 2 SLA Printer) and studied for a controlled release profile of BBR (Choudhury et al., 2021). In recent years microneedles are gaining recognition for their ability to deliver macromolecules like insulin through the skin. However, manufacturing of these structures is complicated and time-consuming as the conventional methods use mold technology.

Although there are various 3D printing technologies, only those that offer high resolution will be suitable for developing microneedles (Sharma et al., 2022). SLA is one such technology that fabricates with great precision. It allows more complex geometries with a size as small as needle tips, as depicted in Fig. 4. Yadav et al. (2021) printed hollow microneedles (HMNs) array using class-I biocompatible resin (Dental SG from Formlabs) as a printing material for the delivery of rifampicin using SLA 3D printer (Form 2 3D printer). The morphology of HMNs comprised sub-apical holes, perpendicular to the needle tip's direction. The height and diameter of the HMNs were maintained at 1150 μm and 950 μm, respectively. While the reservoir volume of HMNs was 360 μL. The optical microscopy and electron microscopy were used to ensure print quality and uniformity across the array. The *ex vivo* permeation across the porcine skin revealed efficient permeation of rifampicin and *in vivo* studies in SD rats showed efficient penetration and desired bioavailability (Yadav et al., 2021). Economidou et al. (2019) printed spear and pyramid-shaped microneedle patches of 15*15*1 mm through SLA (Form 2 SLA printer) by using biocompatible resin (Dental SG from Formlabs) as a printing material for intradermal delivery of insulin. The base dimensions of the printed spear-shaped microneedle were 0.08*1 mm, while for the pyramid-shaped microneedle it was 1*1 mm. The height of both types of microneedles was 1 mm. The surface of these microneedles was coated with insulin in sugar alcohol or disaccharide carriers using inkjet printing. The coating films firmly adhered to the microneedle surface even after the penetration, which was observed through micro-CT analysis. *In vivo* studies revealed lower levels of glucose due to rapid insulin action within 60 min when compared to 4 h by subcutaneous injections (Economidou et al., 2019). Uddin et al. (2020) fabricated 3D printed microneedle arrays for the efficient delivery of cisplatin for treating A-431 epidermoid skin tumors, as shown in Fig. 5. They printed microneedles with 1*1 mm dimensions using SLA (Form 2 SLA printer) and coated them with cisplatin formulations using inkjet dispensing. Franz cell diffusion studies showed fast release rates of cisplatin (80–90%) in 1 h and *in vivo* testing performed on Balb/c nude mice revealed sufficient absorbency of cisplatin and showed high anticancer activity and tumor regression (Uddin et al., 2020).

These studies demonstrated the development of a drug-loaded microneedle array that involves two different steps. The first step is fabricating the microneedle array alone, followed by the incorporation of the drug separately. This approach is time-consuming and uneconomical when compared to the microneedles that are fabricated in a single step by directly incorporating the drug into the photopolymer resin. Lu et al. (2015) developed dacarbazine microneedles by incorporating the API into the PPF and diethyl fumarate solutions. Each microneedle is comprised of a cylindrical base and a conical tip maintained at the height of 700 μm and 300 μm respectively. Whereas the diameter of the cylindrical base was 200 μm and for the conical tip it was 20 μm. The release characteristics revealed the extended release of API for five weeks (Lu et al., 2015). Overall, these studies imply the effectiveness of SLA in precisely fabricating microneedles and other topical/transdermal devices adopting either a single or a multi-step process.

5.3. Implants

An implant is an artificial object or tissue placed in the human body by surgical procedure or simple insertion. They are either temporary or permanent devices intended to serve the functions of failed/missing tissues or organs and can also be used to release the drug. For these implants to achieve high efficacy, they must cater to the needs of a patient, *i.e.*, it must be patient specific. For that reason, there is a high demand for the development of personalized implants. Developing these personalized implants using conventional manufacturing methods can be tedious. However, 3D printing technology has the potential to satiate these requirements. The SLA is highly favorable in fabricating personalized implants owing to its short printing times, high resolution, heat-free printing, and smooth surface finish. In addition, drug-eluting implants are also fabricated to deliver the drug at a controlled rate. Various 3D-printed implants that were fabricated using SLA are presented here.

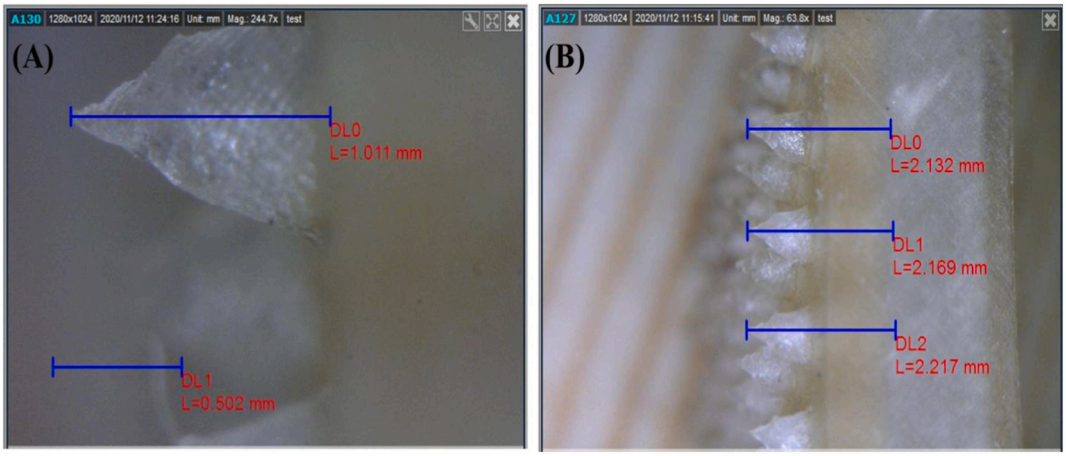

Fig. 4. Microneedles fabricated using SLA illustrating the printing efficiency in terms of dimensions. Reproduced from (Yadav et al., 2021). Copyright: 2021 International Journal of Pharmaceutics.

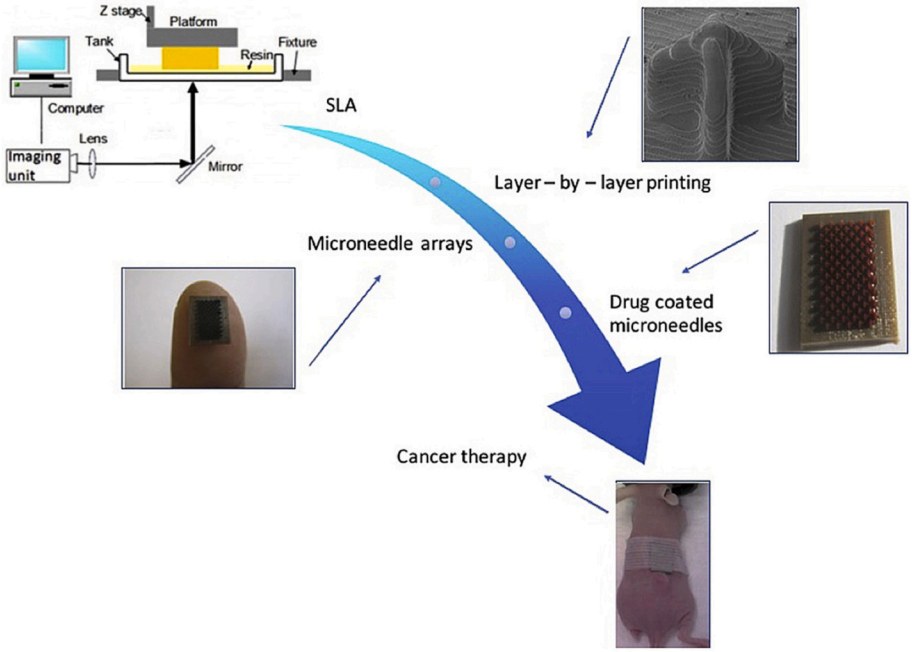

Fig. 5. SLA fabricated Microneedles, process, and application. Reproduced from (Uddin et al., 2020). Copyright: 2019 Materials Science and Engineering: C.

Xu et al. (2021c) developed novel bladder devices (hollow and solid) as depicted in Fig. 6, using SLA 3D printing (Form 2 SLA printer) and elastic Resin from Formlabs as a printing material. They printed solid (length – 130 mm and diameter – 3 mm) and hollow devices (length – 130 mm, outer diameter – 3 mm, shell thickness – 0.5 mm, the diameter of pore openings– 1 mm), where solid devices were prepared by incorporating the drug directly into the resin, while the hollow devices were first printed and later filled with API + Gelucire 48/16 formulation. These bladder devices were incorporated with three different drug loadings of lidocaine hydrochloride (10% *w*/w, 30% w/w, and 50% *w*/w) for a sustained and localized delivery to the urinary bladder, which is used to treat interstitial cystitis and bladder pain. The printed devices showed great flexibility under stretching and retained their original shape after insertion. Hollow devices released the drug completely within four days, whereas solid devices took 2 weeks (Xu et al., 2021c). Drug-eluting ear implants by employing SLA 3D printing technology (Form 2 SLA printer) were developed by Triacca et al. (2022). These implants were designed to target local drug delivery to the ear. Various implant geometries were designed by considering the complexity of the ear anatomy and were 3D printed using flexible resin as printing material loaded with 0.5% *w/v* of Levofloxacin. The *in vitro* drug diffusion studies were performed in a phosphate buffer solution and the results demonstrated that the drug diffusion from the implants was 35 to 50% for 3 weeks (Triacca et al., 2022). These studies illustrated the utility of SLA in the efficient development of implants.

5.4. *Tissue engineering*

3D printing technology, because of its preciseness and structural control over three dimensions from macro to micro scale, can print functional organs or tissues from cells to replace the damaged tissue or to act as a model for drug testing (Dubey et al., 2020; Richards et al., 2013). SLA has wide applications in the field of fabricating supporting structures. For instance, Heo et al. (2019), developed a

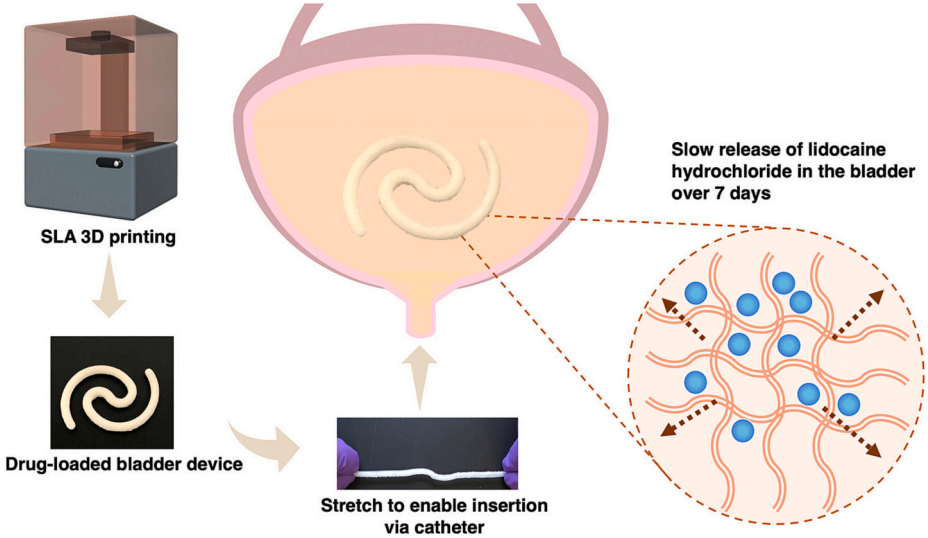

Fig. 6. SLA fabricated urinary bladder device insert. Reproduced from (Xu et al., 2021c). Copyright: 2020 Materials Science and Engineering: C.

photocrosslinkable conductive hydrogel scaffold using a table-top SLA 3D printer (Solidoodle®) for neural tissue engineering. Different concentrations of poly(3,4-ethylenedioxythiophene) (PEDOT): polystyrene sulfonate (PSS) were incorporated to achieve enhanced electrical conductivity. A solution containing PEGDA and bis(2,4,6-trimethylbenzoyl)-phenylphosphineoxide (photoinitiator) was used for photocrosslinking. The 3D-printed scaffolds were well fabricated with the desired geometries and had minimal cytotoxic effects. This research showed that 3D-printed conductive hydrogel with electric stimulation improved the neuronal cell differentiation (Heo et al., 2019). This suggests that SLA 3D printing can be widely employed in bioelectrical applications.

Guillaume et al. (2020) developed a patient-specific implant (PSI) using SLA 3D printing (EnvisionTec Perfactory3® SXGA+) and biodegradable poly (trimethylene carbonate) (PTMC) incorporated with 40% wt. of hydroxyapatite (called Osteo-PTMC) as a printing material, for the orbital floor (OF) repair. This was developed as an alternative to titanium mesh implants. *In vivo* studies showed that Osteo-PTMC led to fast neovascularization and bone morphogenesis in OF region (Guillaume et al., 2020). Alexander et al. (2021) used alumina (Al2O3) ceramic paste for printing four different macroporous ceramic bone implants using SLA 3D printing technology (Ceramaker 900 SLA 3D Printer). The printed implants were 9.2 mm in length and has a 4 mm diameter, intended to resemble trabecular bone. Upon application of high loads, the 3D printed implants exhibited similar compression strength as trabecular bone, making them a good substitute for bone (Safonov et al., 2020). These studies demonstrated the utility of SLA's high resolution and accuracy in the advancement of tissue engineering.

5.5. Dental applications

SLA has been widely explored for dental applications, especially in the fabrication of prosthetics. In 2015, FDA approved the first light-cured resin called Dentca™ Denture Base II, which was intended to be used in the fabrication and restoration of dentures and baseplates (Xu et al., 2021d). Followed by this, in 2017 the FDA approved class II 3D printing resin called NextDent™ Denture for producing denture bases (Chen et al., 2021). Ever since, the market has witnessed widespread biocompatible resins owing to several applications in the manufacturing of drilling templates, dental models, temporary crowns, and bridges. Though various 3D printing technologies, SLA has been profoundly utilized for dental applications because of its high resolution and accuracy. This has been proven by Liang et al. (2018), who developed and compared mouthguards produced through FDM 3D printing with SLA technology. The ones produced through SLA showed higher printing resolution, efficient fitting, and more patient comfort (Liang et al., 2018). Apart from the approved resins, various resins and combinations are being studied for their potential use in dental applications. For instance, Piedra-Cascón et al. (2021) fabricated an occlusal device by incorporating 2 different photosensitive resins using the vat-photopolymerization SLA technique. Flexible resin material comprised the occlusal device's engraved surface, whereas hard resin material comprised the outer surface of the device. This unique design has many advantages, including increased patient compliance, good occlusal distribution forces, and decreased adjustments on engraved surfaces to achieve a better fit (Piedra-Cascón et al., 2021). Similarly, Yue et al. (2015) demonstrated the applications of antimicrobial resins composed of diurethanedimethacrylate, glycerol dimethacrylate, and quaternary ammonium methacrylate in developing dental and orthopedics devices using SLA 3D printing technology (Yue et al., 2015).

5.6. Miscellaneous

In addition to the dosage forms, there are several other innovative drug delivery systems that were fabricated using SLA. Some of those are nasal devices, hearing aids, *etc*. Because of the superior fabrication properties of SLA 3D printing, developing patient-specific devices and implants can be achieved in a short span. Especially, hearing aids fabricated using SLA are persuasive. EnvisionTEC is a leading company that develops personalized hearing aids and ear prosthetics and has biomedically approved printing materials (Hollister and Bergman, 2004). Apart from the commercially available resins, several other novel biocompatible materials have been investigated for their potential to be used in the SLA.

6. Drawbacks

6.1. Safety concerns associated with the materials used in SLA

Despite numerous advantages, the safety concern of SLA-printed pharmaceuticals is a significant drawback since most of the polymers used for SLA are not approved by FDA. (Deshmane et al., 2021). The toxicity of some of the materials used in SLA 3D printing is shown in Table 2. As mentioned above, acrylate-based monomers are an excellent choice in photopolymerization for the development of various pharmaceutical and biomedical products. However, the unreacted monomers present in the final product tend to undergo various chemical reactions under physiological conditions such as hydrolysis (forms acrylic acid and decreases the local pH) and Michael addition reaction (amino or thiol groups of biologically active biomacromolecules) causing irritation and cytotoxicity. In addition, the degradation of polymerized methacrylate leads to the formation of polymethacrylic acid causing inflammation (Husár et al., 2014). Further, the unreacted monomers present in the final dosage form can trigger allergic reactions. The *in vivo* studies on zebrafish embryos revealed the increased survival rates of embryos after eliminating the unreacted monomers (Mostafavi et al., 2021). Therefore, the traces of unreacted monomers must be prevented.

The post-washing and post-curing methods are used to eliminate the unreacted monomers in the final product. The post-washing method uses solvents to remove the unreacted monomers from the final printed dosage form. The most preferred washing solvent is Isopropyl alcohol (IPA), which washes out the uncured monomers. The post-washing process is unsuitable for the drug-loaded 3D structures, as there is a risk of washing away the drug in unreacted monomers affecting the therapeutic efficiency (Xu et al., 2021a). After the post-washing, post-curing is employed, eliminating the unreacted monomers, and providing a smooth surface finish. But this may lead to increased cross-linking density affecting the drug release from the formulation (Wang et al., 2021; Xu et al., 2021a). The monomer conversion rate is not always 100% and can be quantified by using different spectroscopical techniques. In a study conducted by Anastasio et al. (2019), UV-curing causes a decrease in the aliphatic carbon-carbon double bond at 1637 cm^{-1} as shown in Fig. 7, simultaneously increasing the aromatic carbon-carbon bond at 1610 cm^{-1} (Anastasio et al., 2019). Similarly, various other analytical techniques like Raman spectroscopy, solid-state nuclear magnetic resonance, and differential scanning calorimetry can be used to determine the extent of polymerization. In addition, the traces of unreacted photoinitiators (0.1–10%) are far more potent compared to uncured monomers (5–90%) (Detamornrat et al., 2022). No studies found related to removing these materials from the finished products. These unreacted photoinitiators are assumed to be removed by the same post-processing techniques as reported for eliminating monomers.

Besides the toxicity concerns of unreacted monomers, the reaction between the drug and monomers can affect both the toxicity and drug release from the fabricated dosage form. This issue arises when the drug is incorporated directly into the liquid monomers for printing a drug-loaded structure. In a recent study by Xu et al. (2020), the team encountered an unexpected reaction (Michael addition reaction) between amlodipine and PEGDA. The Michael addition reaction occurred between the primary amine group of amlodipine and the diacrylate group of photopolymers (PEGDA) (Xu et al., 2020). Therefore, it is of

Table 2
Toxicological information of photoinitiators, photopolymers, and UV curing agent-photoinitiator. Adapted from © 2022, Detamornrat et al. Small published by Wiley-VCH GmbH (Carve and Wlodkowic, 2018; Detamornrat et al., 2022).

Function	Compound or trade name	Concentration [w/w]	Toxicological information
Photoinitiator	Phosphine oxide compounds (Type II)	0.1–5%	LD_{50} Oral rat - > 5000 mg kg^{-1} LC_{50} (48 h) *Oryzias latipes* - 6.53 mg L^{-1}
	Hydroxy-acetophenone (Type II)	N/A	LD_{50} Oral Rat - 2.240 mg kg^{-1} LC_{50} (96 h) Salmo gairdneri - 25 mg L^{-1}
	Benzophenone compounds (Type II) including benzophenone-3 (BP-3) and benzophe	<10%	LC_{50} (96 h) *Pimephales promelas* - 14.2 mg L^{-1} BP-3 and BP-4: LC_{50} (48 h) *Daphnia magna* - 1.09 and 47.47 mg L^{-1}
	1-hydroxy cyclo hexyl phenyl ketone (Irgacure 184)	N/A	LC_{50} (96 h) *Danio rerio* - 24 mg L^{-1}
Photopolymer	Acrylate monomers, acrylate and urethane acrylate oligomers	5–60%	LD_{50} Oral rat - > 5000 mg kg^{-1} LC_{50} (96 h) *Cyprinus carpio* - 1.2 mg L^{-1} LC_{50} (96 h) *Pimephales promelas* - 34.7 mg L^{-1}
	Methyl methacrylate monomers and oligomers	5–90%	LC_{50} (96 h) *Cyprinodon variegatus* - 1.1 mg L^{-1} LC_{50} (96 h) *Lepomis macrochirus* - 283 mg L^{-1}
	Tripropylene glycoldiacrylate	N/A	LD_{50} oral rat - 7900 mg kg^{-1} LD_{50} oral rat - 6800 mg kg^{-1} LC_{50} (96 h) *Leuciscus idus* - > 4.6–10 mg L^{-1}
	3,4-Epoxycyclohexylmethyl 3,4-epoxy-cyclohexanecarboxylate	25–60%	LC_{50} (96 h) *Oncorhynchus mykiss* - 24 mg L^{-1} LC_{50} oral rats - 5000 mg kg^{-1}
	1,6-bis(2,3-epoxypropoxy) hexane	15–30%	LC_{50} (96 h) *Leuciscus idus* - 30 mg L^{-1} LD_{50} oral rats - 2190 mg kg^{-1}
	Tetraacrylate	30–60%	LC_{50} (96 h) Cyprinus carp - 1.2 mg L^{-1} LC_{50} (96 h) *Danio rerio* - 7.9 mg L^{-1}

utmost importance to study the stability of the drug when intending to mix it with the monomers for printing.

6.2. Unintended raise in temperatures

It is well known that the SLA is suitable for 3D printing thermolabile drugs (Lloyd et al., 1986). However, the temperature may raise above the intended levels during printing due to the exothermic nature of the photopolymerization reaction and may even arise from the light source (Hori et al., 2019). When measured, the exothermic heat can raise the temperature to around 55 °C (CDRH, 2022). In addition, the temperatures around the resin tank can also increase. This may be critical if the thermolabile drugs are incorporated into the monomers for preparing the dosage form. Nevertheless, no reports support drug degradation or product-related problems concerning these unintended temperatures (Xu et al., 2021a).

6.3. Regulatory limitations

In 2017, the FDA issued guidelines on the Technical Considerations for Additive Manufactured Devices. These guidelines focus on the design, materials, software processing, printing process parameters, post-processing parameters, and process validation of 3D-printed medical products. It also outlines the quality issues of the printed product, like description, mechanical properties, dimensions, material chemistry, and biocompatibility (Rahman et al., 2018). However, no guidance document was issued regarding 3D-printed pharmaceutical products. One could expect guidance to be issued in the future potentially with more stringent regulations than medical devices. Unlike conventional products, in which FDA did not focus much on the process while approving the drug product, the regulations for 3D printed pharmaceuticals are expected to include in-process controls. These issues would keep pharmaceutical companies interested in implementing 3D printer technology on hard turf. Further, the lack of concordance between different regulatory bodies adds more burden to manufacturers to satisfy the different sets of guidelines associated with different regulatory agencies. Therefore, it is necessary to bridge the gap between regulatory bodies to ease the process for manufacturers and bring this technology into clinical practice benefiting both manufacturers and consumers (Rahman et al., 2018; Xu et al., 2021a).

Regarding SLA printing, various photopolymerizable resins used in dental prosthetics have been approved by the FDA, but none have been approved for pharmaceutical use. It is predicted that the approval of photopolymerizable resins for pharmaceuticals would be more stringent and independent of a specific product.

7. Conclusion and future prospects

It has been around three decades since the inception of 3D printing technology, and ever since, the industrial world has witnessed significant transformations. It is prevalent in various industries ranging from aerospace, animation, dental, and fashion to jewelry making. Its introduction to the healthcare sector is still in its infancy due to several unanswered concerns associated with this technology. However, several pieces of research prove its high potential in the healthcare system. Therefore, introducing this technology to clinical practice can bring about a digital transformation, restructuring the design of medicines and manufacturing systems. Among several superior vat-photopolymerization technologies, SLA is the oldest and is widely used owing to its affordability (economical), ease of operation, good feature resolution, smooth surface finish, and ability to fabricate complex structures making it highly suitable for developing novel and advanced dosage forms, drug-eluting systems, medical devices, and tissue scaffolds. However, at present, SLA is only confined to fabricating dental prosthetics, which soon can extend its applications to clinical pharmaceutical development.

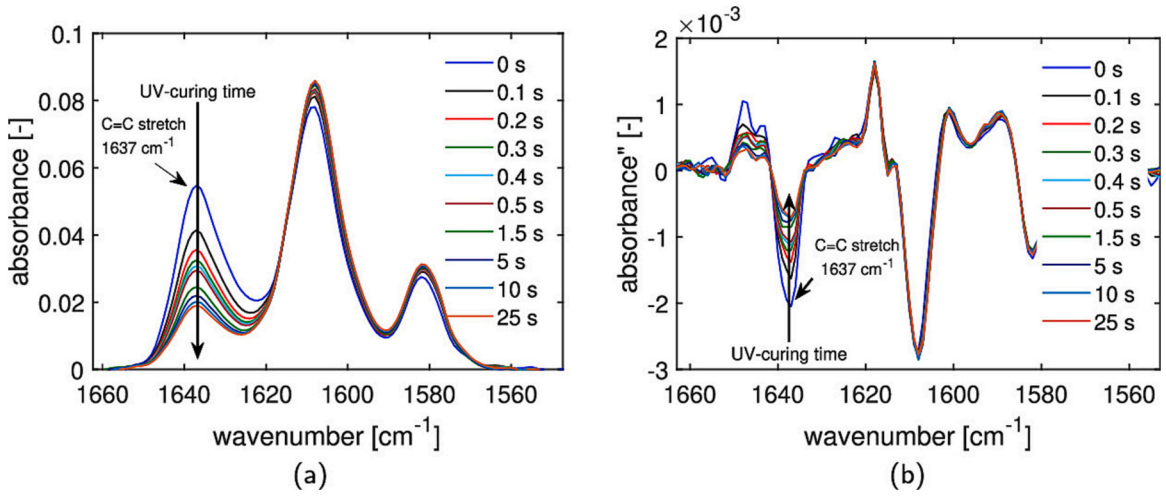

Fig. 7. Evolution of the C=C stretch peak at 1637 cm–1 during UV-curing of the methacrylate resin: absorbance spectra acquired in ATR mode (a) and second derivative of the absorbance (b) as a function of wavenumber. Reproduced from © 2019 American Chemical Society (Anastasio et al., 2019).

SLA can be combined with 3D scanning technology to fabricate patient-specific prosthetics or drug-eluting devices. The 3D scanning technology allows scanning of the topography of the organ or tissue which converts to a digital file that is compatible with being printed using SLA. Scanning-based 3D fabrication is currently employed in developing patient-specific dental prosthetics. For this reason, the efficacy of treatment at the specific site and patient adherence can be achieved. This technology could further be integrated with several smart materials to achieve time-specific drug release and shape memory (4D printing) functionalities. This system can also be utilized in various stages of drug development, from pre-clinical to clinical practice. For instance, its ability to print various sizes and shapes enables it to produce doses suitable for various animal testing models. Similarly, in clinical trials, it can be used to produce placebos and dosage forms with the same structural parameters intended for blindfolded studies. In addition, using this technology in pre-clinical and clinical trials can substantially reduce production costs.

Although mass production of 3D-printed medicines is not feasible, its potential in fabricating novel pharmaceuticals should not be ignored. This technology must be widely explored and deeply investigated to make the 3D printing of pharmaceutical dosage forms a reality. The significant challenges stopping SLA from healthcare applications is the availability of photocurable biomaterials and toxicity concerns associated with them. However, this can be overcome by extensively exploring various photocurable novel materials with biocompatibility and biodegradability. Moreover, as commercial 3D printers do not abide by Good Manufacturing Practice (GMP) requirements, it poses great difficulty to meet the standards of medical agencies. In conclusion, the full potential of SLA 3D printing in pharmaceuticals can be seen only after the successful unraveling of all these challenges, which can make it to clinical practice. Addressing these issues would one day transform health care, where a physician, pharmacist, or dentist could fabricate personalized dosage forms or devices that cater to a patient's needs, at the convenience of their own clinics.

Funding

This review did not receive any specific grants from funding agencies in the public, commercial or not-for-profit sectors.

CRediT authorship contribution statement

Preethi Lakkala: Writing – original draft, Writing – review & editing. **Siva Ram Munnangi:** Conceptualization, Writing – original draft, Writing – review & editing. **Suresh Bandari:** Conceptualization, Writing – review & editing. **Michael Repka:** Writing – review & editing, Resources, Supervision.

Declaration of Competing Interest

The authors declare that they have no known competing financial interests or personal relationships that could have appeared to influence the work reported in this paper.

Data availability

No data was used for the research described in the article.

References

Alexander, A.E., Wake, N., Chepelev, L., Brantner, P., Ryan, J., Wang, K.C., 2021. A guideline for 3D printing terminology in biomedical research utilizing ISO/ASTM standards. 3D Print. Med. 7, 8. https://doi.org/10.1186/s41205-021-00098-5.

Anastasio, R., Peerbooms, W., Cardinaels, R., van Breemen, L.C.A., 2019. Characterization of ultraviolet-cured methacrylate networks: from photopolymerization to ultimate mechanical properties. Macromolecules 52, 9220–9231. https://doi.org/10.1021/acs.macromol.9b01439.

Awad, A., Fina, F., Goyanes, A., Gaisford, S., Basit, A.W., 2020. 3D printing: principles and pharmaceutical applications of selective laser sintering. Int. J. Pharmaceut. 586, 119594 https://doi.org/10.1016/J.IJPHARM.2020.119594.

Bagheri, A., Jin, J., 2019. Photopolymerization in 3D printing. ACS Appl. Polym. Mater. 1, 593–611. https://doi.org/10.1021/ACSAPM.8B00165.

Balakrishnan, H.K., Badar, F., Doeven, E.H., Novak, J.I., Merenda, A., Dumée, L.F., Loy, J., Guijt, R.M., 2020. 3D printing: an alternative microfabrication approach with unprecedented opportunities in design. Anal. Chem. 93, 350–366. https://doi.org/10.1021/ACS.ANALCHEM.0C04672.

Bandari, S., Nyavanandi, D., Dumpa, N., Repka, M.A., 2021. Coupling hot melt extrusion and fused deposition modeling: critical properties for successful performance. Adv. Drug Deliv. Rev. 172, 52–63. https://doi.org/10.1016/J.ADDR.2021.02.006.

Bikas, H., Stavropoulos, P., Chryssolouris, G., 2016. Additive manufacturing methods and modelling approaches: a critical review. Int. J. Adv. Manuf. Technol. 83, 389–405. https://doi.org/10.1007/s00170-015-7576-2.

Burke, G., Devine, D.M., Major, I., 2020. Effect of stereolithography 3D printing on the properties of PEGDMA hydrogels. Polym. 12, 2015. https://doi.org/10.3390/POLYM12092015.

Carve, M., Wlodkowic, D., 2018. 3D-printed chips: compatibility of additive manufacturing photopolymeric substrata with biological applications. Micromachines 9, 91. https://doi.org/10.3390/mi9020091.

Caudill, C., Perry, J.L., Iliadis, K., Tessema, A.T., Lee, B.J., Mecham, B.S., Tian, S., DeSimone, J.M., 2021. Transdermal vaccination via 3D-printed microneedles induces potent humoral and cellular immunity. Proc. Natl. Acad. Sci. 118, e2102595118 https://doi.org/10.1073/pnas.2102595118.

CDRH, 2022. Technical Considerations for Additive Manufactured Medical Devices Guidance for Industry and Food and Drug Administration Staff Preface Public Comment.

Chai, X., Chai, H., Wang, X., Yang, J., Li, J., Zhao, Y., Cai, W., Tao, T., Xiang, X., 2017. Fused deposition modeling (FDM) 3D printed tablets for intragastric floating

delivery of domperidone. Sci. Rep. 71 (7), 1–9. https://doi.org/10.1038/s41598-017-03097-x.
Charoo, N.A., Barakh Ali, S.F., Mohamed, E.M., Kuttolamadom, M.A., Ozkan, T., Khan, M.A., Rahman, Z., 2020. Selective laser sintering 3D printing – an overview of the technology and pharmaceutical applications. Httpsdoi-Orgumissidmoclcorg 46, 869–877. https://doi.org/10.1080/03639045.2020.1764027.
Chen, G., Xu, Y., Kwok, P.C.L., Kang, L., 2020. Pharmaceutical applications of 3D printing. Addit. Manuf. 34, 101209 https://doi.org/10.1016/J.ADDMA.2020.101209.
Chen, H., Cheng, D.-H., Huang, S.-C., Lin, Y.-M., 2021. Comparison of flexural properties and cytotoxicity of interim materials printed from mono-LCD and DLP 3D printers. J. Prosthet. Dent. 126, 703–708. https://doi.org/10.1016/j.prosdent.2020.09.003.
Chia, H.N., Wu, B.M., 2015. Recent advances in 3D printing of biomaterials. J. Biol. Eng. 9, 1–14. https://doi.org/10.1186/S13036-015-0001-4/FIGURES/7.
Chou, W.H., Gamboa, A., Morales, J.O., 2021. Inkjet printing of small molecules, biologics, and nanoparticles. Int. J. Pharmaceut. 600, 120462 https://doi.org/10.1016/J.IJPHARM.2021.120462.
Choudhury, D., Sharma, P.K., Suryanarayana Murty, U., Banerjee, S., 2021. Stereolithography-assisted fabrication of 3D printed polymeric film for topical berberine delivery: in-vitro, ex-vivo and in-vivo investigations. J. Pharm. Pharmacol. https://doi.org/10.1093/JPP/RGAB158.
Daly, R., Harrington, T.S., Martin, G.D., Hutchings, I.M., 2015. Inkjet printing for pharmaceutics – a review of research and manufacturing. Int. J. Pharmaceut. 494, 554–567. https://doi.org/10.1016/J.IJPHARM.2015.03.017.
Deshmane, S., Kendre, P., Mahajan, H., Jain, S., 2021. Stereolithography 3D printing technology in pharmaceuticals: a review. Drug Dev. Ind. Pharm. 47 https://doi.org/10.1080/03639045.2021.1994990.
Detamornrat, U., McAlister, E., Hutton, A.R.J., Larrañeta, E., Donnelly, R.F., 2022. The role of 3D printing technology in microengineering of microneedles. Small 18, 2106392. https://doi.org/10.1002/smll.202106392.
Dubey, S.K., Alexander, A., Sivaram, M., Agrawal, M., Singhvi, G., Sharma, S., Dayaramani, R., 2020. Uncovering the diversification of tissue engineering on the emergent areas of stem cells. Nanotechnol. Biomater. Curr. Stem Cell Res. Ther. 15 https://doi.org/10.2174/1574888X15666200103124821.
Durga Prasad Reddy, R., Sharma, V., 2020. Additive manufacturing in drug delivery applications: a review. Int. J. Pharmaceut. 589, 119820 https://doi.org/10.1016/J.IJPHARM.2020.119820.
Economidou, S.N., Pere, C.P.P., Reid, A., Uddin, M.J., Windmill, J.F.C., Lamprou, D.A., Douroumis, D., 2019. 3D printed microneedle patches using stereolithography (SLA) for intradermal insulin delivery. Mater. Sci. Eng. C Mater. Biol. Appl. 102, 743–755. https://doi.org/10.1016/J.MSEC.2019.04.063.
El Aita, I., Rahman, J., Breitkreutz, J., Quodbach, J., 2020. 3D-printing with precise layer-wise dose adjustments for paediatric use via pressure-assisted microsyringe printing. Eur. J. Pharm. Biopharm. 157, 59–65. https://doi.org/10.1016/J.EJPB.2020.09.012.
Gibson, I., Rosen, D., Stucker, B., 2015. Additive manufacturing technologies: 3D printing, rapid prototyping, and direct digital manufacturing, second edition. In: Addit. Manuf. Technol. 3D Print. Rapid Prototyp. Direct Digit. Manuf. Second Ed. 1–498. https://doi.org/10.1007/978-1-4939-2113-3.
Goole, J., Amighi, K., 2016. 3D printing in pharmaceutics: a new tool for designing customized drug delivery systems. Int. J. Pharmaceut. 499, 376–394. https://doi.org/10.1016/J.IJPHARM.2015.12.071.
Gueche, Y.A., Sanchez-Ballester, N.M., Cailleaux, S., Bataille, B., Soulairol, I., 2021. Selective laser sintering (SLS), a new chapter in the production of solid oral forms (SOFs) by 3D printing. Pharm. 13, 1212. https://doi.org/10.3390/PHARMACEUTICS13081212.
Guillaume, O., Geven, M.A., Varjas, V., Varga, P., Gehweiler, D., Stadelmann, V.A., Smidt, T., Zeiter, S., Sprecher, C., Bos, R.R.M., Grijpma, D.W., Alini, M., Yuan, H., Richards, G.R., Tang, T., Qin, L., Yuxiao, L., Jiang, P., Eglin, D., 2020. Orbital floor repair using patient specific osteoinductive implant made by stereolithography. Biomaterials 233, 119721. https://doi.org/10.1016/J.BIOMATERIALS.2019.119721.
Hagan, C.T., Bloomquist, C., Warner, S., Knape, N.M., Kim, I., Foley, H., Wagner, K.T., Mecham, S., DeSimone, J., Wang, A.Z., 2022. 3D printed drug-loaded implantable devices for intraoperative treatment of cancer. J. Control. Release 344, 147–156. https://doi.org/10.1016/j.jconrel.2022.02.024.
Hahn, V., Kiefer, P., Frenzel, T., Qu, J., Blasco, E., Barner-Kowollik, C., Wegener, M., 2020. Rapid assembly of small materials building blocks (Voxels) into large functional 3D metamaterials. Adv. Funct. Mater. 30, 1907795. https://doi.org/10.1002/adfm.201907795.
He, L., Song, X., 2018. Supportability of a high-yield-stress slurry in a new stereolithography-based ceramic fabrication process. JOM 70, 407–412. https://doi.org/10.1007/s11837-017-2657-3.
He, L., Fei, F., Wang, W., Song, X., 2019. Support-free ceramic stereolithography of complex overhanging structures based on an elasto-viscoplastic suspension feedstock. ACS Appl. Mater. Interfaces 11, 18849–18857. https://doi.org/10.1021/ACSAMI.9B04205/SUPPL_FILE/AM9B04205_SI_001.PDF.
Heo, D.N., Lee, S.-J., Timsina, R., Qiu, X., Castro, N.J., Zhang, L.G., 2019. Development of 3D printable conductive hydrogel with crystallized PEDOT:PSS for neural tissue engineering. Mater. Sci. Eng. C 99, 582–590. https://doi.org/10.1016/j.msec.2019.02.008.
Hollister, S.J., Bergman, T.L., 2004. Chapter 6 Biomedical Applications of Integrated Additive/Subtractive Manufacturing.
Hori, M., Fujimoto, K., Asakura, M., Nagase, Y., Mieki, A., Kawai, T., 2019. Measurement of exothermic heat released during polymerization of a lightcuring composite resin: comparison of light irradiation modes. Dent. Mater. J. 38, 646–653. https://doi.org/10.4012/DMJ.2018-158.
Hsiao, W.K., Lorber, B., Reitsamer, H., Khinast, J., 2017. 3D printing of oral drugs: a new reality or hype?, 15, 1–4. https://doi.org/10.1080/17425247.2017.1371698.
Huang, B., Han, L., Wu, B., Chen, H., Zhou, W., Lu, Z., 2020a. Application of Bis[2-(3,4-epoxycyclohexyl)ethyl] octamethyltetrasiloxane in the Preparation of a Photosensitive Resin for Stereolithography 3D Printing. J. Wuhan Univ. Technol.-Mater Sci. Ed. 346 (34), 1470–1478. https://doi.org/10.1007/S11595-019-2215-7.
Huang, J., Qin, Q., Wang, J., 2020b. A review of stereolithography: processes and systems. Process 8, 1138. https://doi.org/10.3390/PR8091138.
Hull, C.W., Arcadia, C., 1984. Apparatus for Production of Three-Dimensional Objects by Stereolithography.
Husár, B., Hatzenbichler, M., Mironov, V., Liska, R., Stampfl, J., Ovsianikov, A., 2014. 6 - Photopolymerization-based additive manufacturing for the development of 3D porous scaffolds. In: Dubruel, P., Van Vlierberghe, S. (Eds.), Biomaterials for Bone Regeneration. Woodhead Publishing, pp. 149–201. https://doi.org/10.1533/9780857098104.2.149.
Jacob, S., Nair, A.B., Patel, V., Shah, J., 2020. 3D Printing technologies: recent development and emerging applications in various drug delivery systems. AAPS PharmSciTech 21. https://doi.org/10.1208/S12249-020-01771-4.
Kade, M.J., Burke, D.J., Hawker, C.J., 2010. The power of thiol-ene chemistry. J. Polym. Sci. Part Polym. Chem. 48, 743–750. https://doi.org/10.1002/POLA.23824.
Karakurt, I., Aydoğdu, A., Çıkrıkcı, S., Orozco, J., Lin, L., 2020. Stereolithography (SLA) 3D printing of ascorbic acid loaded hydrogels: a controlled release study. Int. J. Pharmaceut. 584, 119428 https://doi.org/10.1016/J.IJPHARM.2020.119428.
Kozhevnikov, A., Kunnen, R.P.J., van Baars, G.E., Clercx, H.J.H., 2020. Influence of the recoating parameters on resin topography in stereolithography. Addit. Manuf. 34, 101376 https://doi.org/10.1016/J.ADDMA.2020.101376.
Lapin, S.C., Snyder, J.R., Sitzmann, E.V., Plaines, D., Barnes, D.K., Green, G.D., 1994. Stereolithography Using Vinyl Ether-Epoxide Polymers.
Lee, K.W., Wang, S., Fox, B.C., Ritman, E.L., Yaszemski, M.J., Lu, L., 2007. Poly (propylene fumarate) bone tissue engineering scaffold fabrication using stereolithography: effects of resin formulations and laser parameters. Biomacromolecules 8, 1077–1084. https://doi.org/10.1021/BM060834V.
Lee, K.-S., Kim, R.H., Yang, D.-Y., Park, S.H., 2008. Advances in 3D nano/microfabrication using two-photon initiated polymerization. Prog. Polym. Sci. 33, 631–681. https://doi.org/10.1016/j.progpolymsci.2008.01.001.
Lee, J., Yi, H., Lee, S., Park, H., Choi, K., Kim, D., 2017. Synthesis of UV-Curable Modified (3,4-epoxycyclohexane)methyl 3,4-epoxycyclohexylcarboxylate acrylate. Korean J. Mater. Res. 27, 199–205. https://doi.org/10.3740/MRSK.2017.27.4.199.
Lewis, J.A., Gratson, G.M., 2004. Direct writing in three dimensions. Mater. Today 7, 32–39. https://doi.org/10.1016/S1369-7021(04)00344-X.
Li, Z., Wang, C., Qiu, W., Liu, R., 2019. Antimicrobial Thiol–ene–acrylate photosensitive resins for DLP 3D printing. Photochem. Photobiol. 95, 1219–1229. https://doi.org/10.1111/PHP.13099.
Lian, Q., Yang, F., Xin, H., Li, D., 2017. Oxygen-controlled bottom-up mask-projection stereolithography for ceramic 3D printing. Ceram. Int. 43, 14956–14961. https://doi.org/10.1016/J.CERAMINT.2017.08.014.
Liang, K., Carmone, S., Brambilla, D., Leroux, J.C., 2018. 3D printing of a wearable personalized oral delivery device: a first-in-human study. Sci. Adv. 4 https://doi.org/10.1126/SCIADV.AAT2544.
Ligon, S.C., Liska, R., Stampfl, J., Gurr, M., Mülhaupt, R., 2017. Polymers for 3D printing and customized additive manufacturing. Chem. Rev. 117, 10212–10290. https://doi.org/10.1021/ACS.CHEMREV.7B00074.
Lloyd, C.H., Joshi, A., McGlynn, E., 1986. Temperature rises produced by light sources and composites during curing. Dent. Mater. 2, 170–174. https://doi.org/10.1016/S0109-5641(86)80030-6.
Lu, Y., Mantha, S.N., Crowder, D.C., Chinchilla, S., Shah, K.N., Yun, Y.H., Wicker, R.B., Choi, J.W., 2015. Microstereolithography and characterization of poly(propylene fumarate)-based drug-loaded microneedle arrays. Biofabrication 7. https://doi.org/10.1088/1758-5090/7/4/045001.
Manapat, J.Z., Chen, Q., Ye, P., Advincula, R.C., 2017. 3D printing of polymer nanocomposites via stereolithography. Macromol. Mater. Eng. 302, 1600553. https://doi.org/10.1002/MAME.201600553.
Martinez, P.R., Goyanes, A., Basit, A.W., Gaisford, S., 2018. Influence of geometry on the drug release profiles of stereolithographic (SLA) 3D-printed tablets. AAPS PharmSciTech 19, 3355–3361. https://doi.org/10.1208/S12249-018-1075-3.
Menditto, E., Orlando, V., De Rosa, G., Minghetti, P., Musazzi, U.M., Cahir, C., Kurczewska-Michalak, M., Kardas, P., Costa, E., Lobo, J.M.S., Almeida, I.F., 2020. Patient centric pharmaceutical drug product design—the impact on medication adherence. Pharm. 12, 44. https://doi.org/10.3390/PHARMACEUTICS12010044.
Meyer, W., Engelhardt, S., Novosel, E., Elling, B., Wegener, M., Krüger, H., 2012. Soft polymers for building up small and smallest blood supplying systems by stereolithography. J. Funct. Biomater. 3, 257–268. https://doi.org/10.3390/JFB3020257.
Mitteramskogler, G., Gmeiner, R., Felzmann, R., Gruber, S., Hofstetter, C., Stampfl, J., Ebert, J., Wachter, W., Laubersheimer, J., 2014. Light curing strategies for lithography-based additive manufacturing of customized ceramics. Addit. Manuf. 1–4, 110–118. https://doi.org/10.1016/J.ADDMA.2014.08.003.
Mostafavi, D., Methani, M.M., Piedra-Cascón, W., Zandinejad, A., Revilla-León, M., 2021. Influence of the rinsing postprocessing procedures on the manufacturing accuracy of vat-polymerized dental model material. J. Prosthodont. 30, 610–616. https://doi.org/10.1111/JOPR.13288.
O'Brien, A.K., Bowman, C.N., 2006. Impact of oxygen on photopolymerization kinetics and polymer structure. Macromolecules 39, 2501–2506. https://doi.org/10.1021/ma051863l.

Palaganas, J., de Leon, A.C., Mangadlao, J., Palaganas, N., Mael, A., Lee, Y.J., Lai, H.Y., Advincula, R., 2017. Facile preparation of photocurable siloxane composite for 3D printing. Macromol. Mater. Eng. 302, 1600477. https://doi.org/10.1002/MAME.201600477.

Pan, Y., He, H., Xu, J., Feinerman, A., 2017. Study of separation force in constrained surface projection stereolithography. Rapid Prototyp. J. 23, 353–361. https://doi.org/10.1108/RPJ-12-2015-0188/FULL/XML.

Park, B.J., Choi, H.J., Moon, S.J., Kim, S.J., Bajracharya, R., Min, J.Y., Han, H.K., 2019. Pharmaceutical applications of 3D printing technology: current understanding and future perspectives. J. Pharm. Investig. 49, 575–585. https://doi.org/10.1007/S40005-018-00414-Y/FIGURES/3.

Patel, D.K., Sakhaei, A.H., Layani, M., Zhang, B., Ge, Q., Magdassi, S., 2017. Highly stretchable and UV curable elastomers for digital light processing based 3D printing. Adv. Mater. 29, 1606000. https://doi.org/10.1002/ADMA.201606000.

Pereira, R.F., Bártolo, P.J., 2015. 3D photo-fabrication for tissue engineering and drug delivery. Engineering 1, 090–112. https://doi.org/10.15302/J-ENG-2015015.

Piedra-Cascón, W., Krishnamurthy, V.R., Att, W., Revilla-León, M., 2021. 3D printing parameters, supporting structures, slicing, and post-processing procedures of vat-polymerization additive manufacturing technologies: a narrative review. J. Dent. 109, 103630 https://doi.org/10.1016/j.jdent.2021.103630.

Plamadeala, C., Gosain, S.R., Hischen, F., Buchroithner, B., Puthukodan, S., Jacak, J., Bocchino, A., Whelan, D., O'Mahony, C., Baumgartner, W., Heitz, J., 2019. Bio-inspired microneedle design for efficient drug/vaccine coating. Biomed. Microdevices 22, 8. https://doi.org/10.1007/s10544-019-0456-z.

Prasad, L.K., Smyth, H., 2015. 3D printing technologies for drug delivery: a review. Orgumissidmoclcorg 42, 1019–1031. https://doi.org/10.3109/03639045.2015.1120743.

Prasher, A., Shrivastava, R., Dahl, D., Sharma-Huynh, P., Maturavongsadit, P., Pridgen, T., Schorzman, A., Zamboni, W., Ban, J., Blikslager, A., Dellon, E.S., Benhabbour, S.R., 2021. Steroid eluting esophageal-targeted drug delivery devices for treatment of eosinophilic esophagitis. Polymers 13, 557. https://doi.org/10.3390/polym13040557.

Quan, H., Zhang, T., Xu, H., Luo, S., Nie, J., Zhu, X., 2020. Photo-curing 3D printing technique and its challenges. Bioact. Mater. 5, 110–115. https://doi.org/10.1016/j.bioactmat.2019.12.003.

Rahman, Z., Barakh Ali, S.F., Ozkan, T., Charoo, N.A., Reddy, I.K., Khan, M.A., 2018. Additive manufacturing with 3D printing: progress from bench to bedside. AAPS J. 206 (20), 1–14. https://doi.org/10.1208/S12248-018-0225-6.

Raman, R., Bashir, R., 2015. Stereolithographic 3D bioprinting for biomedical applications. Essent. 3D Biofabric. Transl. 89–121. https://doi.org/10.1016/B978-0-12-800972-7.00006-2.

Richards, D.J., Tan, Y., Jia, J., Yao, H., Mei, Y., 2013. 3D printing for tissue engineering. Isr. J. Chem. 53, 805–814. https://doi.org/10.1002/IJCH.201300086.

Robles-Martinez, P., Xu, X., Trenfield, S.J., Awad, A., Goyanes, A., Telford, R., Basit, A. W., Gaisford, S., 2019. 3D printing of a multi-layered polypill containing six drugs using a novel stereolithographic method. Pharm. 11, 274. https://doi.org/10.3390/PHARMACEUTICS11060274.

Rodríguez-Pombo, L., Xu, X., Seijo-Rabina, A., Ong, J.J., Alvarez-Lorenzo, C., Rial, C., Nieto, D., Gaisford, S., Basit, A.W., Goyanes, A., 2022. Volumetric 3D printing for rapid production of medicines. Addit. Manuf. 52, 102673 https://doi.org/10.1016/j.addma.2022.102673.

Safonov, A., Maltsev, E., Chugunov, S., Tikhonov, A., Konev, S., Evlashin, S., Popov, D., Pasko, A., Akhatov, I., 2020. Design and fabrication of complex-shaped ceramic bone implants via 3d printing based on laser stereolithography. Appl. Sci. Switz. 10, 1–18. https://doi.org/10.3390/APP10207138.

Sangermano, M., Duarte, M.L.B., Ortiz, R.A., Gómez, A.G.S., Valdez, A.E.G., 2010. Diol spiroorthocarbonates as antishrinkage additives for the cationic photopolymerization of bisphenol-A–diglycidyl ether. React. Funct. Polym. 70, 98–102. https://doi.org/10.1016/J.REACTFUNCTPOLYM.2009.10.010.

Scoutaris, N., Ross, S., Douroumis, D., 2016. Current trends on medical and pharmaceutical applications of inkjet printing technology. Pharm. Res. 338 (33), 1799–1816. https://doi.org/10.1007/S11095-016-1931-3.

Seo, H., Heo, S.G., Lee, H., Yoon, H., 2017. Preparation of PEG materials for constructing complex structures by stereolithographic 3D printing. RSC Adv. 7, 28684–28688. https://doi.org/10.1039/C7RA04492E.

Seoane-Viaño, I., Ong, J.J., Luzardo-Álvarez, A., González-Barcia, M., Basit, A.W., Otero-Espinar, F.J., Goyanes, A., 2021. 3D printed tacrolimus suppositories for the treatment of ulcerative colitis. Asian J. Pharm. Sci. 16, 110–119. https://doi.org/10.1016/j.ajps.2020.06.003.

Sharma, P.K., Choudhury, D., Yadav, V., Murty, U.S.N., Banerjee, S., 2022. 3D printing of nanocomposite pills through desktop vat photopolymerization (stereolithography) for drug delivery reasons. 3D Print. Med. 81 (8), 1–10. https://doi.org/10.1186/S41205-022-00130-2.

Smith, P.J., Morrin, A., 2017. CHAPTER 1:Reactive Inkjet Printing—An Introduction 1–11. https://doi.org/10.1039/9781788010511-00001.

Steinbach, M., Gartz, M., Hirsch, R., 2020. Design and characterization of 3D printable photopolymer resin containing poly(2-hydroxyethyl methacrylate) for controlled drug release. J. Drug Deliv. Sci. Technol. 59, 101850 https://doi.org/10.1016/J.JDDST.2020.101850.

Sumerel, J., Lewis, J., Doraiswamy, A., Deravi, L.F., Sewell, S.L., Gerdon, A.E., Wright, D. W., Narayan, R.J., 2006. Piezoelectric ink jet processing of materials for medical and biological applications. Biotechnol. J. 1, 976–987. https://doi.org/10.1002/BIOT.200600123.

Taormina, G., Sciancalepore, C., Messori, M., Bondioli, F., 2018. 3D printing processes for photocurable polymeric materials: technologies, materials, and future trends. J. Appl. Biomater. Funct. Mater. 16, 151–160. https://doi.org/10.1177/2280800018764770.

Thakkar, R., Pillai, A.R., Zhang, J., Zhang, Y., Kulkarni, V., Maniruzzaman, M., 2020. Novel on-demand 3-Dimensional (3-D) printed tablets using fill density as an effective release-controlling tool. Polymers 12. https://doi.org/10.3390/POLYM12091872.

Tomal, W., Ortyl, J., 2020. Water-soluble photoinitiators in biomedical applications. Polymers 12. https://doi.org/10.3390/POLYM12051073.

Triacca, A., Pitzanti, G., Mathew, E., Conti, B., Dorati, R., Lamprou, D.A., 2022. Stereolithography 3D printed implants: a preliminary investigation as potential local drug delivery systems to the ear. Int. J. Pharmaceut. 616, 121529 https://doi.org/10.1016/J.IJPHARM.2022.121529.

Tumbleston, J.R., Shirvanyants, D., Ermoshkin, N., Janusziewicz, R., Johnson, A.R., Kelly, D., Chen, K., Pinschmidt, R., Rolland, J.P., Ermoshkin, A., Samulski, E.T., DeSimone, J.M., 2015. Continuous liquid interface production of 3D objects. Science 347, 1349–1352. https://doi.org/10.1126/SCIENCE.AAA2397/SUPPL_FILE/TUMBLESTON.SM.PDF.

Uddin, M.J., Scoutaris, N., Economidou, S.N., Giraud, C., Chowdhry, B.Z., Donnelly, R.F., Douroumis, D., 2020. 3D printed microneedles for anticancer therapy of skin tumours. Mater. Sci. Eng. C Mater. Biol. Appl. 107, 110248 https://doi.org/10.1016/j.msec.2019.110248.

Upul Ranaweera, R.A.A., Schuman, T.P., Wang, R., Miller, B.D., Kilway, K.V., 2015. Effect of moisture on cationic polymerization of silicone epoxy monomers. J. Appl. Polym. Sci. 132 https://doi.org/10.1002/APP.41831.

Vivero-Lopez, M., Xu, X., Muras, A., Otero, A., Concheiro, A., Gaisford, S., Basit, A.W., Alvarez-Lorenzo, C., Goyanes, A., 2020. Anti-biofilm multi drug-loaded 3D printed hearing aids. Mater. Sci. Eng. C Mater. Biol. Appl. 119, 111606. https://doi.org/10.1016/J.MSEC.2020.111606.

Wang, J., Goyanes, A., Gaisford, S., Basit, A.W., 2016. Stereolithographic (SLA) 3D printing of oral modified-release dosage forms. Int. J. Pharmaceut. 503, 207–212. https://doi.org/10.1016/J.IJPHARM.2016.03.016.

Wang, X., Schmidt, F., Hanaor, D., Kamm, P.H., Li, S., Gurlo, A., 2019. Additive manufacturing of ceramics from preceramic polymers: a versatile stereolithographic approach assisted by thiol-ene click chemistry. Addit. Manuf. 27, 80–90. https://doi.org/10.1016/J.ADDMA.2019.02.012.

Wang, J., Zhang, Y., Aghda, N.H., Pillai, A.R., Thakkar, R., Nokhodchi, A., Maniruzzaman, M., 2021. Emerging 3D printing technologies for drug delivery devices: current status and future perspective. Adv. Drug Deliv. Rev. 174, 294–316. https://doi.org/10.1016/J.ADDR.2021.04.019.

Weems, A.C., Arno, M.C., Yu, W., Huckstepp, R.T.R., Dove, A.P., 2021. 4D polycarbonates via stereolithography as scaffolds for soft tissue repair. Nat. Commun. 121 (12), 1–14. https://doi.org/10.1038/s41467-021-23956-6.

Wen, H., Jung, H., Li, X., 2015. Drug delivery approaches in addressing clinical pharmacology-related issues: opportunities and challenges. AAPS J. 17, 1327. https://doi.org/10.1208/S12248-015-9814-9.

Windolf, H., Chamberlain, R., Quodbach, J., 2021. Predicting drug release from 3D printed oral medicines based on the surface area to volume ratio of tablet geometry. Pharmaceutics 13, 1453. https://doi.org/10.3390/PHARMACEUTICS13091453/S1.

Xu, X., Robles-Martinez, P., Madla, C.M., Joubert, F., Goyanes, A., Basit, A.W., Gaisford, S., 2020. Stereolithography (SLA) 3D printing of an antihypertensive polyprintlet: case study of an unexpected photopolymer-drug reaction. Addit. Manuf. 33, 101071 https://doi.org/10.1016/J.ADDMA.2020.101071.

Xu, X., Awad, A., Robles-Martinez, P., Gaisford, S., Goyanes, A., Basit, A.W., 2021a. Vat photopolymerization 3D printing for advanced drug delivery and medical device applications. J. Control. Release 329, 743–757. https://doi.org/10.1016/J.JCONREL.2020.10.008.

Xu, X., Awwad, S., Diaz-Gomez, L., Alvarez-Lorenzo, C., Brocchini, S., Gaisford, S., Goyanes, A., Basit, A.W., 2021b. 3D printed punctal plugs for controlled ocular drug delivery. Pharmaceutics 13, 1421. https://doi.org/10.3390/pharmaceutics13091421.

Xu, X., Goyanes, A., Trenfield, S.J., Diaz-Gomez, L., Alvarez-Lorenzo, C., Gaisford, S., Basit, A.W., 2021c. Stereolithography (SLA) 3D printing of a bladder device for intravesical drug delivery. Mater. Sci. Eng. C Mater. Biol. Appl. 120 https://doi.org/10.1016/J.MSEC.2020.111773.

Xu, X., Seijo-Rabina, A., Awad, A., Rial, C., Gaisford, S., Basit, A.W., Goyanes, A., 2021d. Smartphone-enabled 3D printing of medicines. Int. J. Pharmaceut. 609, 121199 https://doi.org/10.1016/j.ijpharm.2021.121199.

Yadav, V., Sharma, P.K., Murty, U.S., Mohan, N.H., Thomas, R., Dwivedy, S.K., Banerjee, S., 2021. 3D printed hollow microneedles array using stereolithography for efficient transdermal delivery of rifampicin. Int. J. Pharmaceut. 605, 120815 https://doi.org/10.1016/J.IJPHARM.2021.120815.

Yogesh, P., Richa, P., Chandrashekhar, N.S., Karunakaran, K.P., 2020. Layer Separation Mechanisms in DLP 3D Printing 179–187. https://doi.org/10.1007/978-981-32-9433-2_15.

Yue, J., Zhao, P., Gerasimov, J.Y., Van De Lagemaat, M., Grotenhuis, A., Rustema-Abbing, M., Van Der Mei, H.C., Busscher, H.J., Herrmann, A., Ren, Y., 2015. 3D-printable antimicrobial composite resins. Adv. Funct. Mater. 25, 6756–6767. https://doi.org/10.1002/ADFM.201502384.

Zakeri, S., Vippola, M., Levänen, E., 2020. A comprehensive review of the photopolymerization of ceramic resins used in stereolithography. Addit. Manuf. 35, 101177 https://doi.org/10.1016/J.ADDMA.2020.101177.

Zhang, J., Vo, A.Q., Feng, X., Bandari, S., Repka, M.A., 2018. Pharmaceutical additive manufacturing: a novel tool for complex and personalized drug delivery systems. AAPS PharmSciTech 19, 3388. https://doi.org/10.1208/S12249-018-1097-X.

Zhao, Z., Kuang, X., Yuan, C., Qi, H.J., Fang, D., 2018. Hydrophilic/hydrophobic composite shape-shifting structures. ACS Appl. Mater. Interfaces 10, 19932–19939. https://doi.org/10.1021/ACSAMI.8B02444/SUPPL_FILE/AM8B02444_SI_003.MPG.

Zhao, Z., Tian, X., Song, X., 2020. Engineering materials with light: recent progress in digital light processing based 3D printing. J. Mater. Chem. C 8, 13896–13917. https://doi.org/10.1039/D0TC03548C.

Zheng, Y., Deng, F., Wang, B., Wu, Y., Luo, Q., Zuo, X., Liu, X., Cao, L., Li, M., Lu, H., Cheng, S., Li, X., 2021. Melt extrusion deposition (MEDTM) 3D printing technology – a paradigm shift in design and development of modified release drug products. Int. J. Pharmaceut. 602, 120639 https://doi.org/10.1016/j.ijpharm.2021.120639.